

Quantitative evaluation and intercomparison of morning and afternoon MODIS aerosol measurements from Terra and Aqua Satellites

Charles Ichoku^{1,2}, Lorraine A. Remer², and Thomas F. Eck^{3,4}

¹Science Systems and Applications Inc., Lanham, Maryland

²Laboratory for Atmospheres, NASA/Goddard Space Flight Center, code 913, Greenbelt, Maryland

³Laboratory for Terrestrial Physics, NASA/Goddard Space Flight Center, code 923, Greenbelt, Maryland

⁴Goddard Earth Sciences and Technology (GEST) Center, University of Maryland - Baltimore County, Baltimore, Maryland

In press:

Journal of Geophysical Research, JGR

Special Issue on: “Global Aerosol System”

Submission Date : 04 May 2004

Revision Date : 01 July 2004

Acceptance Date : 05 July 2004

Abstract

The quality of the aerosol optical thickness (AOT) data retrieved operationally from MODIS sensors aboard the Terra and Aqua satellites, over land and ocean, from 2000 to 2003 (Aqua only from June 2002), were evaluated thoroughly, and the utility and synergisms of the two sensors in retrieving aerosols for global, regional, and local applications were examined. Because of periodic updates of the MODIS aerosol algorithm, a series of data versions have been produced and distributed, and those currently in wide circulation are Terra-MODIS versions 3 and 4 data (T003 and T004) and Aqua-MODIS version 3 data (A003); though the algorithm version used to retrieve T004 and A003 was almost the same. These three data sets (T003, T004, and A003) were evaluated independently and comparatively with collocated AOT from ground-based AERONET sun photometers. The analysis shows that at 550 nm wavelength, 67.3%, 55.0%, and 55.5% of AOT from T003, T004, and A003, respectively, meet the pre-specified accuracy conditions of $\pm(0.05 + 0.2aot)$ over land, while about 63.3%, 59.4%, and 62.2%, respectively, fall within the more stringent range of $\pm(0.03 + 0.05aot)$ over ocean. However, when based on equal standards of comparison and regression analysis, aerosol retrievals are much more accurate over ocean than over land. Both MODIS and AERONET AOTs at 550 nm collocated over AERONET stations were grouped into three aerosol size modes based on AERONET Angstrom exponent value ranges, and time series of their monthly averages at Terra overpass times show that there is a net increase in the monthly average loading of the large size mode aerosols from 2000 to 2003, especially over ocean. Note that this trend was based only on data over AERONET sites, and does not represent the full global statistics. Analysis of MODIS full regional AOT averages from 12 land and 6 oceanic regions, shows that aerosol loading exhibits an annual cycle in almost every region, with the exception of very remote oceanic regions such as the Central Pacific. On the basis of regional monthly averages, West Africa, China, and India

show the highest peak monthly mean AOT value of ~ 0.7 at 550 nm, while the highest over-ocean aerosol loading occurs over the Mediterranean and Mid-Atlantic oceans, with a regional monthly peak of ~ 0.35 , which is half of the peak over land. The magnitude of day-to-day variation between morning (Terra) and afternoon (Aqua) AOT varies from region to region, and increases with aerosol loading for any given region. However, none of the regions examined shows any consistent regional trend in morning-to-afternoon aerosol loading; all showing almost equal likelihoods of increase or decrease from morning to afternoon.

1 INTRODUCTION

The Moderate Resolution Imaging Spectroradiometer (MODIS) twin sensors were launched under the auspices of the NASA Earth Observing System (EOS) program: the first on December 18, 1999 aboard the Terra satellite, and the second on May 04, 2002 aboard the Aqua satellite; and have both been measuring reflected and emitted radiance from the earth and the atmosphere, day and night. Terra and Aqua, which are both polar-orbiting satellites, cross the equator during the daytime at approximately 10:30 am (morning) and 1:30 pm (afternoon) local times, respectively. Radiance data are acquired by MODIS in 36 spectral bands, spanning 405 – 14385 nm wavelengths, which range from the visible (VIS) through the near-infrared (NIR) and mid-infrared (MIR) up to the thermal infrared (TIR) regions of the electromagnetic spectrum. They are acquired in one of three spatial resolutions at nadir: 0.25 km (bands 1-2: VIS), 0.5 km (bands 3-7: VIS-MIR), and 1 km (bands 8-36: VIS-TIR). MODIS data are being used operationally to generate a variety of geophysical parameters employed in monitoring the earth's lands, oceans, and atmosphere. The products generated from MODIS are continuously being archived by appropriate NASA data centers and are distributed freely. The algorithms used to generate these

products undergo periodic revisions, and data users are not always sure about the version and quality of the products they are using at any given time. It is, therefore, necessary to conduct periodic calibration and evaluation of the products to keep track of their evolution and make the information available to users.

In this study, focus is on the MODIS aerosol products, which are retrieved at 10-km spatial resolution based on 0.25 and 0.5-km resolution reflectance data, with separate algorithms over land and ocean. The principal aerosol parameter from MODIS is the aerosol optical thickness (AOT or $\tau_{a\lambda}$) retrieved over land at 470 nm and 660 nm wavelengths (then interpolated at 550 nm), and over ocean at 550, 660, 870, 1200, 1600, and 2100 nm (then extrapolated to 470 nm). Other important MODIS aerosol parameters include the proportion (η) of AOT contributed by the aerosol fine mode fraction, Ångström exponent, emitted and reflected fluxes, and aerosol mass concentration -- all derived over land and ocean; as well as aerosol effective radius derived over ocean only. Complete details of the original algorithms and parameters derived over land and/or ocean are given in [*Kaufman et al.*, 1997; *Tanre et al.*, 1997], while the recent updates are described fully in [*Remer et al.*, 2004].

The purpose of evaluation, calibration, and validation is to detect biases, if any, originating from the processes involved in deriving the products, and to establish the accuracy levels of the products, based on comparison with independent observations of known accuracy (ground truth). In the case of measurement of global aerosols, the most well organized and well documented ground truth data sets are those observed under the banner of the AERosol RObotic NETwork (AERONET) and other associated networks (e.g. the Canadian AEROCAN and the French PHOTONS) [*Holben et al.*, 1998, 2001]. This network employs automatic sunphotometers/sky radiometers, which are located at over 100 sites worldwide, and whose data are regularly made

available online by the AERONET team (<http://aeronet.gsfc.nasa.gov/>). Among other optically equivalent aerosol parameters, AOT data are derived from most AERONET Sun photometers at 340, 380, 440, 500, 670, 870, and 1020 nm wavelengths, while a few of their newer instruments also provide AOT at 532, 535, and 1640 nm. AERONET provides highly accurate AOT data, with uncertainty levels in the range of 0.01 to 0.02 (though slightly higher in the ultraviolet wavelengths) [Eck, *et al.* 1999]. Typically, AOT is measured at each AERONET site at least every 15 min during the daytime (under cloud-free conditions). It is, therefore, feasible and necessary to conduct periodic evaluation of the aerosol and other products, from both Terra and Aqua MODIS sensors, in a comparative and comprehensive manner.

Results of early validation activities of the Terra-MODIS aerosol products using AERONET data were reported in [Chu *et al.*, 2002; Ichoku *et al.*, 2002; Remer *et al.*, 2002]. Subsequently, several important data filtering and algorithm improvement strategies and techniques were developed and implemented [Gao *et al.*, 2002; Martins *et al.*, 2002]. Results of some of the initial applications for global and regional studies have been published in [Kaufman *et al.*, 2002; Ichoku *et al.*, 2003; Levy *et al.*, 2003]. Indeed, the aerosol community has long begun using MODIS data quantitatively and extensively for regional and global aerosol pollution assessments, climate forcing calculations, and model comparisons [Christopher and Zhang, 2002; Chu *et al.*, 2003; Yu *et al.*, 2003, Koren *et al.*, 2004]. Details of the latest algorithm status and main changes, as well as longer term validation results from Terra-MODIS have been described in Remer *et al.* [2004]. Although the same aerosol algorithm is used for both Terra and Aqua MODIS processing, thus far, most of the published validation and other studies involving MODIS aerosol products used only Terra data, whereas only limited preliminary assessment has been conducted using aerosol products from Aqua MODIS [Ichoku *et al.*, 2004].

In this paper, focus will be mainly on a comprehensive evaluation of Terra and Aqua MODIS spectral aerosol optical thickness $\tau_{a\lambda}$, which is the most important parameter from which others can be derived. Another major aspect of this study is to use the opportunity afforded by the availability of aerosol data from Terra and Aqua to study the patterns of aerosol distribution in the morning and afternoon. The general design and scope of the current study will be described in section 2. Updated validation activities and results of MODIS $\tau_{a\lambda}$ will be presented in section 3. A discussion of the main application-focused comparisons and synergisms between Terra and Aqua MODIS aerosol products at global, regional, and local scales will be given in section 4. The summary and conclusion will be presented in section 5.

2 DESIGN AND SCOPE OF STUDY

The aim of this investigation is to evaluate the quality of all available aerosol spectral optical thickness, $\tau_{a\lambda}$, generated from MODIS on both Terra and Aqua starting from the onset of data acquisition from each sensor up to the end of 2003. Obviously, this involves the analysis of a huge amount of different versions of data from two sensors covering the entire globe daily, one for almost four years, and the other for almost two years. Therefore, it was necessary to design the study in such a way that the analysis will be well packaged and presented to adequately meet the needs of the scientific community, especially those involved in the quantitative use of the data.

2.1 MODIS and AERONET aerosol data characteristics

The calibrated radiance data from MODIS is classified as level 1B in the processing hierarchy. Algorithms are developed to retrieve geophysical parameters classified as level 2, which when aggregated (spatially, temporally, or both), can be categorized as level 3 or higher. The algorithms used for level 2 aerosol retrieval are, like all other MODIS algorithms, periodically revised and updated. After major algorithm revisions, previously processed data may be reprocessed. As a result, there could be multiple data versions (also internally referred to as data ‘collections’) based on algorithm updates. Thus far, Terra-MODIS aerosol data has had collections 002, 003, and 004. Since collection 002 data were the first version to be generated in the operational production mode, they were basically pre-validation data and were not widely used in applications. On the other hand, collections 003 and 004 have been distributed and used quite substantially. Aqua-MODIS aerosol data started with collection 003, generated with algorithms corresponding to those of Terra-MODIS collections 003 and 004 and intervening minor updates. Aqua-MODIS collection 004 data were just starting to be produced at the time of this study, and were not yet available for analysis. For simplicity in this paper, Terra-MODIS collection 003 and 004 aerosol products will be designated by Terra_V003 (or T003) and Terra_V004 (or T004) respectively, while Aqua-MODIS collection 003 products will be designated by Aqua_V003 (or A003).

AERONET $\tau_{a\lambda}$ data are categorized into three levels of processing, namely: level 1.0 (aerosol data product with only pre-deployment instrument calibration applied), level 1.5 (cloud-screened [Smirnov *et al.*, 2000] level 1.0 data), and level 2.0 (quality assured level 1.5 data, having been checked and adjusted with pre- and post-deployment calibrations). AERONET level 1.5 data are available in near real time, while, depending on site and length of deployment, level

2.0 is only available several weeks to several months behind real time. Therefore, for reasons of expediency, MODIS aerosol validation is performed mostly with AERONET level 1.5 data.

In evaluating MODIS aerosol products with AERONET in certain parts of this paper, the adopted convention for comparison is to subtract AERONET data from corresponding MODIS data and use the resulting “MODIS – AERONET” (or $M-A$) difference to assess the performance of MODIS relative to AERONET. This has been done such that, taking AERONET to be the ground truth, ‘positive’ and ‘negative’ values of these $M-A$ differences will respectively represent ‘over-’estimation and ‘under-’estimation by MODIS.

2.2 Geographic Considerations of Study

Although part of the analysis will be conducted in an integral global fashion, however, given the variability of aerosol regimes, such an analysis alone may not be sufficiently effective in communicating the data quality assessment results. Therefore, to enable a better assessment of regional peculiarities, several large regions were identified such that the study could also be conducted in a comparative way between them. Twelve rectangular regions were selected over land, and six over ocean. Since this work is somewhat driven by evaluation/validation of different aerosol types with AERONET measurements, the distribution of these regions was determined by two factors, namely (i) the main distribution centers of different aerosol types and, (ii) availability of AERONET stations.

Figure 1 shows a map of multi-year average AOT at 550 nm for the period of April 2000 to November 2003, derived from Terra-MODIS global monthly average data sets at 1° spatial resolution. The map was generated using the MODIS Online Visualization and Analysis System (MOVAS), which can be used online at (<http://lake.nascom.nasa.gov/movas/>). The boundaries of

the rectangular regions selected for this study are shown in white; with solid lines for land and dotted lines for ocean. The land regions are labeled with numerals (1 to 12), while the ocean regions are labeled with alphabets (A to F). Table 1 shows the correspondence between the labels and the names of the regions shown in Figure1, as well as coordinates of the box boundaries and the dominant aerosol types in each region. The dominant aerosol type in each region has been determined from literature [Holben *et al.*, 2001; Dubovik *et al.*, 2002, Kaufman *et al.*, 2002; Ichoku *et al.*, 2004; Remer *et al.*, 2004]. ‘Mixed’ is used to designate aerosol types with more than two dominant species (such as combined influence of urban/industrial pollution, smoke, and dust). Most of the regional studies performed in this paper will refer to the regions represented in Figure 1 and Table 1. To facilitate broad zoning in later sections, all regions having at least a negative (-ve) boundary longitude (Min_Lon or Max_Lon) in Table 1 will be classified as Western Hemisphere (WH), while others will be classified as Eastern Hemisphere (EH).

3 MODIS AEROSOL DATA VALIDATION

The validation of MODIS aerosol products is accomplished mainly with the use of equivalent data acquired from the ground based AERONET network. Collocated MODIS and AERONET data are extracted and compared in order to evaluate MODIS accuracy based on that of AERONET, either globally, regionally, or locally. The principle of MODIS and AERONET data sampling were described in detail in Ichoku *et al.* [2002]. However, for completeness in this paper, the process will be summarized in subsection 3.1.

3.1 MODIS and AERONET data sampling for validation

The main difficulty in data sampling from MODIS and AERONET is the differences in their data structures. During each overpass, MODIS covers an extensive area across a given AERONET instrument site almost in an instant, whereas the AERONET sun photometer takes point measurements several times during the daytime. Therefore, whereas MODIS data expresses spatial variability, AERONET data expresses temporal variability. To reconcile these differences in order to achieve a balanced comparison, spatial averages of MODIS pixels falling within a 50x50-km box centered over each AERONET station are taken to compare with temporal averages of AERONET data measured ± 30 min of MODIS overpass time. This equivalence is based on the assumption that, from estimates of Saharan dust transport, air masses transporting aerosol travel a distance of approximately 50 km per hour on the average [*Ichoku et al.*, 2002]. Thus, if a segment of an aerosol plume is imaged by MODIS within a 50x50-km box centered over an AERONET station, it is assumed that part of that aerosol plume segment may have passed over the AERONET station during the 30 min preceding MODIS overpass, while the other part will pass over the station during the 30 min following MODIS overpass. As such, the MODIS and AERONET statistics derived as described here are indeed determined from different samples of the same aerosol population. These MODIS validation statistics are generated quasi-operationally as the MODIS level 2 aerosol products are being produced. One of the conditions adopted for validation with the spatio-temporal averages computed here is that the MODIS statistics would have been computed with at least 5 pixels (out of a maximum of 25 pixels expected in a 50x50-km box) and AERONET statistics would have been computed with at least 2 observations (out of a maximum of 5 observations expected in a period of 1-hour of observations at 15 min time intervals) [*Ichoku et al.* 2002; *Remer et al.*, 2002].

To verify the quality of AERONET level 1.5 $\tau_{a\lambda}$ data for aerosol validation relative to the corresponding level 2.0 (quality assured) data, the AERONET level 1.5 AOT ± 30 min averages for 2000 to 2003 were plotted against corresponding AERONET level 2.0 data at three wavelengths (440, 670, and 870 nm), separately over land and ocean and for Terra and Aqua overpass times. In all cases, there was almost perfect correlation, with coefficient of determination (r^2) ranging from 0.993 to 1, thereby making the correlation coefficients (r) practically always equal to unity. Given this impressive correlation between AERONET levels 1.5 and 2.0 data sets, our confidence is reassured that it is valid to use AERONET level 1.5 $\tau_{a\lambda}$ to validate MODIS $\tau_{a\lambda}$. Nevertheless, it is pertinent to note that, when AERONET level 2.0 data are not available, any errors that may exist in level 1.5 would have no effect, since in a correlation analysis, only points having both data types contribute. In this study, during the evaluation analysis, effort will be made to exclude specific level 1.5 AERONET data known to be unsuitable for validation. That filtering process will be discussed in section 3.2.

MODIS and AERONET wavelengths do not match exactly except at 870 nm. Therefore, to enable comparison at matching wavelengths, AERONET $\tau_{a\lambda}$ used for MODIS validation at 470, 550, and 660 nm are interpolated from AERONET $\tau_{a\lambda}$ at 440 and 870 nm, based on the assumption of uniform spectral dependence between these two wavelengths, represented by the Ångström exponent, α , parameter (Equation 1):

$$\alpha_{870/440} = \frac{\ln(\tau_{a870} / \tau_{a440})}{\ln(870/440)}, \quad (1)$$

where, $\alpha_{870/440}$ is the Ångström exponent based on AOT at 440 and 870 nm wavelengths.

3.2 Evaluation of MODIS data accuracy with AERONET

An important aspect of the preparation activities embarked upon prior to the launch of the first MODIS, was an experimental determination of the range of uncertainties expected from MODIS aerosol retrieval, which for $\tau_{a\lambda}$ were estimated to be $\pm(0.05 + 0.2\tau_{a\lambda})$ over land and $\pm(0.03 + 0.05\tau_{a\lambda})$ over ocean [Kaufman *et al.*, 1997; Tanré *et al.*, 1997]. In each case, the constant term represents the estimated error due to surface reflectance assumptions, while the second term, which is often proportional to $\tau_{a\lambda}$, represents the error due to aerosol model assumptions. The uncertainty in surface reflectance and model assumptions are, obviously, both expected to be larger for land than for ocean. Nevertheless, earlier validation results showed that most of the over-land and over-ocean Terra-MODIS $\tau_{a\lambda}$ data met their respective pre-specified expectations [Chu *et al.*, 2002; Remer *et al.*, 2002; Remer *et al.*, 2004].

3.2.1 Data Assessment and Filtering

In this work, the first step in the evaluation of the MODIS $\tau_{a\lambda}$ with corresponding AERONET level 1.5 data involved computing the relative errors for all collocated data points to determine the *%pass* of MODIS $\tau_{a\lambda}$ (percentage falling within the expected uncertainty) at each AERONET station, in order to identify possible station-specific effects on MODIS performance. Table 2a and 2b list respectively the land and ocean AERONET stations where less than 50% of MODIS τ_{a550} fall within the expected uncertainty; showing the average number of collocated data points (*ndata*) and the average *%pass* (averaged from T003, T004, and A003). A careful examination of the site characteristics enabled the compilation of the probable reasons, why there was such low MODIS/AERONET agreement over each of such stations. The main site-dependent sources of uncertainties over pure land sites include: uncertainty in surface

reflectance assumptions due to the attenuating effects of excessive surface brightness (usually associated with semi-arid and arid regions), urban surface variability, and snow and melting snow in the higher latitudes. All ocean-based AERONET instruments exist on coastal or island locations, with the exception of a few instruments on offshore platforms, which are close to land. Therefore, the main factors affecting ocean sites also affect coastal and island sites, and include: uncertainty in distinguishing land from water especially when the coastline is complex, as well as the attenuating effects of sandy beaches, swamps, marshes, water sediments, and sea ice (in higher latitudes) on measured reflectance. Factors, which can be common to land and ocean sites (coastal or not) include: persistent cloud cover, and possible error in AERONET data due to instrument or other operational problems, and AERONET observation from high altitude mountain peaks not accounting for the lower level aerosols measured by MODIS in the surrounding areas. Furthermore, although collocated samples of MODIS and AERONET used to derive the spatio-temporal averages are assumed to represent the same aerosol population over any given site, differences in the special distribution of aerosol loading can affect the MODIS/AERONET agreement substantially.

In certain situations, AERONET/MODIS collocated data sets are known to be either not properly matched or to contain errors, and the integrity of the evaluation can be compromised by the use of such data. Therefore, although it is practically impossible to identify all such cases, attempt has been made to exclude from the AERONET/MODIS comparisons conducted in this paper those known to fall under such categories. The excluded stations are identified with an 'X' on the first column of Tables 2a and 2b. The excluded stations are not necessarily those that exhibit the least *%pass*. Rather, the following criteria are used for exclusion both over land and ocean: data for periods where AERONET data were known to be erroneous (Ilorin, April 25 to

Aug 30, 2003; Kejimikujik), stations where AERONET instruments are located at very high altitudes (Mauna-Loa), and stations with less than 3 collocated pairs. In this last case (<3 pairs), they are assumed to be either new or temporary stations where the measurement may not be sufficiently characterized, or long-term stations with perpetual (cloud or instrument) problems limiting data acquisition times, with the probability that even the measured data may be contaminated. In addition, over land, offshore stations (COVE, Helgoland, and Venice) are excluded, because it is known that any land within the MODIS 50x50-km box would be marginal, while over ocean, stations known to be located far from actual ocean (Bac_Lieu and CEILAP-BA) are also excluded. Although, many of the other stations may also fall under these categories, they have not been excluded because these unfavorable characteristics were not confirmed in their case.

3.2.2 Integrated Global Evaluation

When the MODIS aerosol products were of limited volume and only from Terra, the evaluation or validation was based on the use of standard scatter plots for regional or global data [Chu *et al.*, 2002; Ichoku *et al.*, 2002; Remer *et al.*, 2002]. The second round of Terra-MODIS validation was conducted with a larger volume of data (two year's worth), and the standard scatter plots were no longer applicable directly. Instead, the data were first aggregated according to value ranges before use in modified scatter plots [Ichoku *et al.*, 2004; Remer *et al.*, 2004]. Given that the data volume has continued to increase, with the addition of Aqua-MODIS and multiple data versions, only the modified scatter plots can be used to graphically express the global correlation in a reasonable way.

The data aggregation process for the generation of modified scatter plots involved the binning of AERONET $\tau_{a\lambda}$, with a uniform class interval of 0.05. For each class, the statistics of

all MODIS data points corresponding to the AERONET data points in that class are calculated to represent the MODIS $\tau_{a\lambda}$ for that class. Figure 2 shows modified scatter plots of MODIS $\tau_{a\lambda}$ class averages against AERONET $\tau_{a\lambda}$ bin center values, separately for T003, T004, and A003, at 470, 550 and 660 nm wavelengths over land, and at 550, 660, and 870 nm over ocean. Only MODIS $\tau_{a\lambda}$ averages computed from at least 3 data points were plotted. The MODIS $\tau_{a\lambda}$ standard deviations are plotted as error bars only for the 550-nm curves (to limit clutter). The dotted diagonal line in each panel is the 1-to-1 line, while the near-diagonal pair of broken lines defines the pre-specified uncertainty envelop $\{\text{land: } \pm(0.05 + 0.2\tau_{a\lambda}), \text{ or ocean: } \pm(0.03 + 0.05\tau_{a\lambda})\}$, which is invariably wider for land than for ocean. The total number of data points (np) used is shown in each graph, while the cumulative counts of data points in each class are plotted at all wavelengths represented. The percent proportion of MODIS τ_{a550} falling within the specified uncertainty bounds in each class are plotted ($\%pass_550$). Over land, MODIS tends to overestimate slightly at low AOT values ($\tau_{a550} < 0.15$ for T003, and $\tau_{a550} < 0.25$ for T004 and A003), with $\sim 60\%$ falling within the uncertainty bounds; but more ($\sim 75\%$) of the individual collocated MODIS retrievals fall within the uncertainty range at moderate aerosol loading; while for the largest AOT values (constituting less than 2% of total retrievals), there is wide fluctuation (probably because the statistics were based on very small samples, with greater spatial and temporal variation in AOT). At low AOT values, the error bars are shorter and the $\%pass_550$ range is larger ($\sim 65\%$) for T003 relative to T004 and A003, probably because of increased uncertainty due to extension of retrieval over brighter surfaces [Remer *et al.*, 2004] in the newer versions (T004 and A003). Over ocean, there is no significant offset at the lowest AOT values, and despite the more stringent error tolerance, most of the MODIS $\tau_{a\lambda}$ class averages fall within the uncertainty boundaries, except at 870 nm where there seems to be slight underestimation for

the largest 5% of the AOT values, probably due to uncertainty in the representation of non-sphericity in the dust model [Remer *et al.*, 2004]. Indeed, whereas the *%pass₅₅₀* exceeds 80% at the lowest AOT values for all the data versions, *%pass₅₅₀* decreases continuously as the AOT values increase, and fluctuates very widely for the largest AOT values (less than 2% of total retrievals).

To obtain an overall quantitative summary of how well MODIS $\tau_{a\lambda}$ data meet the uncertainty expectations and correlate with AERONET $\tau_{a\lambda}$ globally, the percentages of MODIS $\tau_{a\lambda}$ within the uncertainty envelopes and the correlation parameters were computed from the actual (unbinned) MODIS and AERONET $\tau_{a\lambda}$ collocated pairs, for each data set (T003, T004, and A003) over land and ocean, separately using AERONET levels 1.5 and 2.0. Table 3 shows the number of data point pairs N used for computing the parameters for each data set (T003, T004, and A003) and the values of the parameters at different wavelengths. The parameters include: percentages of MODIS $\tau_{a\lambda}$ within the uncertainty bounds (*%pass*), the linear correlation coefficients r , and the slopes and intercepts of the regression lines. Referring to results based on AERONET level 1.5, T003 has larger *%pass* (more data contained within the error bounds) both over land and ocean, and has better r and intercept over land, thereby supporting the theory that the extension of retrieval over brighter surfaces in the later algorithm versions (T004 and A003) introduced greater uncertainty over land (as evidenced by the size of the error bars in the plots of Figure 2). Over ocean, T004 and A003 are better than T003 in terms of r , slope and intercept; showing that the later algorithm versions (T004 and A003) produced overall improvement over ocean. The fact that *%pass* is slightly worse in these later versions may have been caused by differences in the distribution of aerosol types and loading. There appears to be no significant difference, in regards to *%pass*, for using AERONET level 1.5 or 2.0. This is because the act of

filtering out a few erroneous AERONET level 1.5 $\tau_{a\lambda}$ to level 2.0 has very little effect on the *%pass* parameter, which is a simple ratio between two large numbers. However, the use of AERONET level 2.0 $\tau_{a\lambda}$ appears to yield appreciable improvement in the correlation coefficient r , slope, and intercept of the regression line, both over land and ocean, especially for T003, which, being the oldest data set, has the largest proportion of available AERONET level 2.0 $\tau_{a\lambda}$. This improvement shows that MODIS $\tau_{a\lambda}$ data are intrinsically more accurate than they appear to be when validated with the readily available level 1.5 AERONET data, as is often the case.

In summary, based on point-by-point comparison with AERONET, the proportion of MODIS-retrieved AOT falling within the specified uncertainty envelope globally ranges from approximately 50% to 70%, generally increasing with wavelength from 470 to 870 nm, both over land and ocean (see Table 3). However, over land, when based on $\tau_{a\lambda}$ bin averages (as Figure 2 shows), at low aerosol loading (approximately, $\tau_{a550} < 0.20$) MODIS has the tendency to over estimate slightly, at moderate aerosol loading (approximately, $0.20 < \tau_{a550} < 0.70$) MODIS measures more accurately, while for very heavy aerosol loading (approximately, $\tau_{a550} > 0.70$) MODIS accuracy fluctuates unpredictably, with more tendency to underestimation. Over ocean, at low aerosol loading (approximately $\tau_{a550} < 0.20$) MODIS retrieves $\tau_{a\lambda}$ mostly accurately. The accuracy of MODIS retrieval over ocean decreases as aerosol loading increases, although considering that the over-ocean uncertainty tolerance is very stringent and that more than 90% of the cases have relatively low AOT ($\tau_{a550} < 0.40$, as seen with the aid of the cumulative frequency curves in Figure 2), the net accuracy is very high. Overall, by comparing the parameters of the equivalent versions of Terra (T004) and Aqua (A003) $\tau_{a\lambda}$, there does not appear to be any clear difference in performance between them.

3.2.3 Time-varying Regional Evaluation

The aim of this study is not limited to validation for the globe or a specific targeted region based on pre-specified error criteria, but one of the main objectives is to assess the general accuracy of the aerosol products from both Terra and Aqua MODIS in a manner that will be of direct benefit to the user of the products for various applications including long-term climate studies [Remer *et al.*, 2004]. Therefore, effort is made to integrate the stationary, regional, and temporal aspects of this analysis in such a simple way as to enable the user to calculate the level of error potentially involved in using data from the available versions of Terra- or Aqua-MODIS products for a given region and time period. As such, the $M-A$ differences of AOT at 550 nm ($\Delta^{M-A}\tau_{a,550}$) calculated with AERONET level 1.5 data over all sites were grouped into regions, and their regional monthly averages were calculated. Time series plots were generated for these monthly-averaged $\Delta^{M-A}\tau_{a,550}$ values and plotted over the corresponding MODIS average AOT at 550 nm for the different data versions and regions, as shown in Figures 3a,b. The condition for plotting a data point is that its monthly average must have been computed from at least 3 values. For each region, the upper sets of curves represent the regional monthly average $\Delta^{M-A}\tau_{a,550}$, showing whether MODIS agrees with, overestimates, or underestimates AERONET, and by how much; while the lower sets of curves are corresponding time series of the MODIS regional monthly average $\tau_{a,550}$, which serve as reference, showing where the levels of disagreement may depend on the AOT level.

The large data gaps in some regions is because some have only one or just a few AERONET stations, and due to the preponderance of cloudy situations in some regions, it is difficult to obtain the required two AERONET observations within ± 30 min of MODIS overpass. Thus, some of the monthly averages plotted in Figures 3a,b were computed from only one station and

perhaps just a few days, which are certainly not representative of the situation for the region or for the month. In such cases, the errors may appear exaggerated with respect to what a true average derived from a representative sample set would be. However, where qualifying data were found for only a single AERONET station in a given region, the name of that station is shown in the graph.

Figure 4 shows the overall regional average bar chart for the evaluation of MODIS $\tau_{a,550}$ with AERONET level 1.5 $\tau_{a,550}$. The bars represent the average MODIS $\tau_{a,550}$ for each data set (T003, T004, and A003) for the entire period of collocated data availability for this study, while the topping spikes are the corresponding average $\Delta^{M-A}\tau_{a,550}$, which, depending on whether they project above or below the top of the bars, represent MODIS overestimation or underestimation respectively, with respect to AERONET. Tables 4a and 4b show the overall summary of the regional validation over land and ocean, respectively, with the list of AERONET stations whose data were available for this study, and an outline of results for each region based on Figures 3a,b and 4. The generalizations, which can be made from these results include: (i) the over-ocean retrievals show better agreement with AERONET than the over-land retrievals; (ii) for the same satellite and data version there are significant differences in performance between regions; (iii) over ocean, there is little or no difference in performance between T003, T004, and A003 for a given region; (iv) over land, average $\Delta^{M-A}\tau_{a,550}$ for T003 is generally smaller than those of T004 and A003, which show identical performance because the algorithms used in retrieving T004 and A003 were almost identical; (v) regardless of satellite or data version, regions with tendency toward overestimation are all over land and include: NW-America, US-Central, US-East, W-Europe, and India (with an overall average overestimation of the order of 0.05), and China, Middle-East, and Australia (with an overall average overestimation of the order of 0.15).

3.3 Apportionment of Errors in MODIS aerosol data products

A wide variety of checks and verifications are conducted during the development and revisions of MODIS algorithms before they are implemented in the production mode. Nevertheless, given that there are several other factors, which can affect the quality of the products, including sensor calibration, satellite motion and observation geometry, environmental conditions (such as cloud cover or surface brightness and variability) during measurement, ancillary data accuracy, model assumptions, and even unforeseen errors in the algorithm, which may not be obvious in a few test cases, it is important to conduct post-production bulk data checks with a much larger volume of data, particularly with respect to an independent set of measurements such as AERONET data, with a view to identifying the main sources of errors and developing strategies to correct them.

To identify the main sources of errors in the MODIS aerosol products, the individual (not the monthly mean) values of $\Delta^{M-A}\tau_{a,550}$ were directly plotted against different parameters including water vapor and satellite observation geometry parameters in order to investigate possible influences by these parameters. Plots generated against water vapor did not show any major trends or biases. Patterns observed with respect to scattering angle (which incorporates solar zenith and azimuth angles and the sensor zenith and azimuth angles) are different over land and ocean, but there is no obvious dependence on scattering angle. However, plots against the sensor zenith angle, which is directly proportional to scan angle, clearly portrays some dependence.

Figure 5 shows plots of $\Delta^{M-A}\tau_{a,550}$ class means against sensor zenith angle bins (5° class intervals), representing the different versions of MODIS aerosol products (T003, T004 and A003) for land and ocean. The class standard deviations are represented as error bars, shown

only for the Land_T004 and Ocean_T004 to avoid clutter. Overall, there are larger deviations over land than over ocean, because MODIS aerosol products are generally more accurate over ocean [Remer *et al.*, 2004]. The over-land curves are definitely inclined; being more positively biased at lower scan angles, with gradual descent toward the zero-line at larger scan angles. Similar analysis conducted on regional basis show that regions with brighter surfaces (Middle East, Australia, US_Central) or regions with numerous small water bodies or more physical development (US_East, West Europe) show more scan angle dependence than regions with darker or more uniform surfaces (Brazil, Russia, southern Africa). This apparent overestimation by MODIS at smaller scan angles is probably caused by the dominance of the effects of land surface variability [Chu *et al.*, 2002; Ichoku *et al.*, 2002], which diminishes as one moves away from nadir. In an independent study on the role of ‘adjacency effect’ on aerosol remote sensing, it was observed that “contrast of surface scene is the most important factor affecting the accuracy of aerosol retrieval” and “at subkilometer resolution the error of aerosol retrieval due to adjacency effect diminishes for higher off nadir angles” [Lyapustin and Kaufman, 2001, p. 11913]. Although MODIS aerosol products are reported at 10-km spatial resolution, they are retrieved from the 0.25-km and 0.50-km resolution radiance channels. A recent study revealed that the omission of polarized radiative transfer in over-land aerosol retrieval introduces errors in AOT, which can reach up to 0.3 in extreme cases, and can be negative or positive depending on the scattering geometry, but is negligible at nadir and increases with both solar and sensor zenith angles [Levy *et al.*, 2004]. Therefore, the obvious positive bias at small sensor zenith angle over land cannot be due to the polarization effect, but most likely due to surface effects. The over-ocean curves show almost no inclination, but show a slight increase of (both negative and

positive) deviations at very high scan angles. This increase of deviation at very high scan angles may also be present in the over-land data, but may have been obscured by the surface effects.

4 TERRA AND AQUA COMPARISON AND SYNERGISM

MODIS aerosol products are applicable to various types of aerosol studies. Globally and regionally, they can be used to develop aerosol climatology and calculate radiative forcing effects on climate. Locally, they can be used to assess pollution levels and effects on environmental dynamics. The fact that MODIS acquires data both in the morning (Terra) and afternoon (Aqua) makes the dataset particularly strategic for studies involving some diurnal variability assessment, although with average overpass time difference of only ~3 hours (Terra => 10:30, Aqua => 13:30 hours local time), the full diurnal pattern cannot be characterized.

In this section, emphasis will be focused on the relationships and differences between morning (Terra) and afternoon (Aqua) observations, without distinguishing data versions. The Terra data versions (T003 and T004) are not differentiated in this segment of the analysis because, as Figures 3a,b shows, in the data sets used for this research, during the period of availability of A003, there is no overlap between T003 and T004. Thus, combination of the later two, allows for data continuity to match A003 for an appreciable time period. Also, since the focus in this section is ‘morning’ and ‘afternoon’ rather than version differences, and the accuracy of data versions is not significantly different, there is no need to differentiate T003 and T004 for this part of the analysis. Therefore, in the following subsections, all reference to Terra (or morning) will be based on T003 and T004 combined, while references to Aqua (or afternoon) will be based on A003 only.

4.1 Global Aerosol Abundance from Terra and Aqua MODIS

The analysis in this subsection is based on data acquired only over AERONET stations, which spatially does not represent full global sampling. In a study conducted with AERONET data just before the launch of the first MODIS on Terra, *Kaufman et al.* [2000] posed the question: “Will aerosol measurements from Terra and Aqua polar orbiting satellites represent the daily aerosol abundance and properties?”. This question was addressed in that paper, where AERONET data segments observed at predicted Terra and Aqua overpass times were used to represent MODIS observations, and the conclusion was that “Terra and Aqua aerosol measurements can represent the average annual value to within 2% error” [*Kaufman et al.*, 2000, p. 3861]. However, now that actual MODIS data are available, it will be interesting to see if they will reproduce the pattern that AERONET predicted. To do this, average AOT at 470, 550, and 660 nm were calculated from the collocated MODIS/AERONET (50x50 km and ± 30 -min) validation data, separately for MODIS and AERONET, at Terra and Aqua overpass times, over land and ocean. Prior to averaging, Ångström exponent (α) was computed from all AERONET data as defined in equation (1), and AERONET AOT were interpolated at 470, 550, and 660 nm. Then, all data sets were partitioned into three groups on the basis of the range of AERONET Ångström exponents (α) that they fall into ($\alpha < 0.7$, $0.7 < \alpha < 1.8$, or $\alpha > 1.8$). *Kaufman et al.* [2000] indicated that $\alpha < 0.7$ would represent predominantly dust aerosols (large size mode), $\alpha > 1.8$ predominantly pollution or smoke aerosols (small size mode), and $0.7 < \alpha < 1.8$ mixed continental aerosols (medium size range). It should be noted that α was derived by *Kaufman et al.* [2000] using 865 and 550 nm wavelengths, whereas the pair used in this work were 870 and 440 nm because these are the two AERONET wavelengths spanning the three wavelengths (470, 550, 660 nm) upon which this analysis is based.

Figure 6 shows the wavelength dependent plots of the AOT averages from MODIS and AERONET data for the three divisions of Ångström exponents, separately at Terra and Aqua overpass times, over land and ocean (Figure 6a,b,c,&d). One aspect that needs to be highlighted from these global average spectral AOT ($\tau_{a\lambda}$) plots is that, for each α division, considering morning (Terra) and afternoon (Aqua) observations separately, over-land values are markedly higher than their over-ocean counterparts; whereas when over-land and over-ocean plots are considered separately, afternoon (Aqua) average values are slightly higher than corresponding morning (Terra) values. Over land, MODIS overestimates AERONET in all three α divisions, although the difference is least at the $\alpha < 0.7$ division, and less for Terra than for Aqua in the other two divisions. Also, average spectral dependencies from MODIS are not very consistent with those of corresponding AERONET divisions. Over ocean, MODIS and AERONET $\tau_{a\lambda}$ are quite close, but their spectral dependencies are noticeably different, especially for the coarse particle size (dust and sea salt) category ($\alpha < 0.7$). However, when the overall average $\tau_{a\lambda}$ for the three α divisions are calculated and plotted without distinguishing Terra and Aqua or land and ocean (Figure 6e), MODIS is seen to overestimate AERONET by about 0.03 (for the coarse mode dominated aerosol) to 0.06 (for the fine mode dominated aerosol). Therefore, since the global average $\tau_{a\lambda}$ estimated from AERONET at Terra and Aqua overpass times represented the AERONET global daily aerosol abundance accurately [Kaufman *et al.*, 2000], it follows from this analysis that MODIS would overestimate the global average $\tau_{a\lambda}$ by about 0.03 to 0.06, which indeed correspond approximately to MODIS detection limit over land and ocean, based on the pre-specified accuracy ranges of $\pm(0.05 + 0.2\tau_{a\lambda})$ over land and $\pm(0.03 + 0.05\tau_{a\lambda})$ over ocean [Kaufman *et al.*, 1997; Tanré *et al.*, 1997, Chu *et al.*, 2002; Remer *et al.*, 2002, 2004]. It is pertinent to note, however, that most of the data used in this analysis comes from land, where

most AERONET stations are located, whereas most MODIS aerosol retrievals are over ocean, which are much more accurate, implying that fully sampled MODIS global averages would represent the reality much more accurately than the above analysis shows.

To assess the seasonal trends, if any, in the observed MODIS overestimate relative to AERONET, monthly averages of the collocated AOT at 550 nm were derived and plotted for the three divisions of Ångström exponent considered ($\alpha < 0.7$, $0.7 < \alpha < 1.8$, or $\alpha > 1.8$). Figure 7 shows separate time series plots of these averages for Terra and Aqua overpass times, over land and ocean. MODIS and AERONET curves are designated with M(α _range) and A(α _range), respectively. Over land, MODIS shows a systematic overestimation with respect to AERONET in all three groups both at Terra and Aqua overpass times, almost all the time. However, in the large mode ($\alpha < 0.7$) division, AERONET shows higher values than MODIS during some peak (probably dust) events, particularly in the fall season of 2001 and 2003. Over ocean, there is very good agreement between MODIS and AERONET for all three α divisions on both Terra and Aqua, although again the large mode ($\alpha < 0.7$) shows MODIS slightly overestimating AERONET occasionally. One remarkable feature of all curves put together is the seasonality in global concentration of all the aerosol size groups, both in the morning (Terra) and afternoon (Aqua), over land and ocean; with the peak periods being usually around boreal spring to summer, while the troughs are mostly in boreal winter. Also, considering only the Terra plots, which show longer term data, there seems to be a net gradual increase in aerosol loading during the three year period shown (Nov 2000 – Nov 2003). In particular, over ocean, during that time period, the net large mode ($\alpha < 0.7$) loading (probably dust) seems to have almost doubled, both from MODIS and AERONET data, at least in the morning (at Terra overpass time). It is important to specify

that the foregoing net increase is based on data acquired only over AERONET stations, and may not represent the full global aerosol trend.

4.2 Regional Seasonal and Diurnal Aerosol Trends from MODIS

Although the global seasonal and diurnal trends of τ_{a550} have been discussed in the preceding subsection, nevertheless, it is useful to see the differences between the regions (as designated in Figure 1). To achieve a balanced analysis, it is preferable to use regional averages based on full data sampling for each region, as opposed to the use of averages based on just samples taken over a few discrete (AERONET) stations. Therefore, in this section, only regional daily and monthly τ_{a550} averages, derived from all pixels of the daily MODIS level 2 (10-km resolution) aerosol data within each region will be used.

Figure 8 shows the time series of the Terra-MODIS monthly average τ_{a550} plotted for each of the regions, roughly separated into western hemisphere WH land (top panel), eastern hemisphere EH land (middle panel), and ocean (bottom panel). Note that the vertical scale of the ocean panel is twice that of the land plots. With the exception of the Central Pacific, which shows almost no variation over time, all other regions (land and ocean alike) portray moderate to very strong seasonal cycles, although the specific peak and low seasons vary from region to region. Among the WH land regions, West Africa shows by far the highest aerosol loading, with the level of τ_{a550} at its low season generally higher than the maxima over the rest of the western hemisphere regions. This dominance of West Africa is probably because it is situated within the equatorial African biomass-burning belt and is in close proximity to the southern African smoke and Saharan dust source regions. Therefore, it is almost continuously impacted by large volumes of smoke and dust, as well as other aerosols originating from local sources. China and India, both of which top the list in the EH land, are subjected to similar heavy impacts of dust, smoke, and

pollution. The regional monthly mean τ_{a550} range (low-to-peak) for these three regions is approximately 0.3 to 0.7. The Middle East, which experiences high aerosol loading during its intense dust (spring-summer) seasons, settles to very moderate levels in winter, with a range of ~ 0.2 to 0.6 . The major biomass burning regions: Brazil, Russia, and Southern Africa have comparable but moderate seasonal peak levels, with a range of ~ 0.1 to 0.4 . The industrialized regions of West Europe and North American (NW_America, US_Central, and US_East) have not only the same aerosol loading, but also follow the same spring-summer high to winter low seasonal cycle, with a range of ~ 0.1 to 0.3 , although NW_America is the least typical. Australia shows a range of ~ 0.1 to 0.25 . Over ocean, the Mediterranean Sea and the Mid-Atlantic Ocean, because of their nearness to Saharan dust sources, dominate over other oceanic regions, and have approximately the same level of aerosol loading and seasonal cycle, with a range of ~ 0.15 to 0.35 . Therefore, the regional monthly mean τ_{a550} range over these two most heavily loaded oceanic regions is about half that of the most heavily loaded land regions (West Africa, China, and India). The Asian Pacific Ocean reflects the impact of Asian continental dust and biomass burning, with a range of ~ 0.15 to 0.25 , while the Southern Atlantic and North Indian Oceans display the effects of their nearness to southern African smoke and Indian mixed aerosol regions respectively, with a range of ~ 0.1 to 0.2 . Central Pacific remains the overall cleanest region with a low and slim range of ~ 0.08 to 0.12 , because it is the most remote of all regions from land where the major aerosol sources are located. It is pertinent to mention that the dust-dominated regions in Figure 8 do not show the type of increasing trend seen in Figure 7 (for the dust category) probably because Figure 8 plots are based on MODIS full spatial sampling (as opposed to just over AERONET sites) and include all aerosol types and size ranges in each region (as opposed to just the large particle group).

Knowledge of the diurnal variation of aerosol loading is very important in many areas of application and, using AERONET data, *Smirnov et al.* [2002] showed that major urban/industrial centers exhibit the greatest diurnal cycle, with a variation of 10-40% during the day at most sites. Although the twice-a-day aerosol observation offered by MODIS (approx. 10:30 and 13:30 hr local times) may not allow full characterization of the diurnal patterns in aerosol loading, however, the morning-to-afternoon variation for each region can be examined using the differences between the Terra (morning) and Aqua (afternoon) regional daily τ_{a550} averages. Figures 9a,b show the time series plots of the Terra-MODIS daily average τ_{a550} (lower points, left scale) co-plotted with the corresponding (Aqua – Terra) τ_{a550} differences (upper points, right scale) for each of the study regions. These regional daily mean (Aqua – Terra) τ_{a550} differences will be denoted by $D^{A-T}\tau_{a550}$ for convenience in the rest of this section. Terra is subtracted from Aqua, such that positive and negative differences will represent morning-to-afternoon increase and decrease, respectively. The plots cover the period of co-existence of Terra and Aqua (June 2002 to November 2003) within the period of this study (February 2000 to November 2003). Table 5 shows the overall average of the $D^{A-T}\tau_{a550}$ values plotted in Figures 9a,b for each region for the entire time period represented. These overall average regional (Aqua – Terra) difference of AOT at 550 nm will, for easy reference, be designated by $Avg^{A-T}\tau_{a550}$, in the rest of this discussion. One feature that needs to be pointed out in Figures 9a,b is the enhanced positively biased differences in the plots for NW_America, US_Central, US-East, and Russia in February/March 2003, which resulted in the elevation of the overall mean $Avg^{A-T}\tau_{a550}$ for these regions ($0.018 < Avg^{A-T}\tau_{a550} < 0.063$). This situation was caused by melting snow contamination in Aqua-MODIS, whose cloud/snow mask was initially inadequate until it was corrected after that season. Other than that known situation, surprisingly, the $D^{A-T}\tau_{a550}$ points for every region appear

to be almost symmetrically distributed about the zero line for both land and ocean. The amplitude of the day-to-day variation of $D^{A-T}\tau_{a550}$ in each region (i.e. the vertical point spread) is proportional to that of the corresponding τ_{a550} at any given time period. However, based on $Avg^{A-T}\tau_{a550}$, there is a small net morning-to-afternoon increase over land regions, except over West Africa, though the margin is very small ($-0.012 < Avg^{A-T}\tau_{a550} < 0.020$). The over-ocean regions show almost equal likelihood of increasing or decreasing with a very tiny margin ($-0.005 < Avg^{A-T}\tau_{a550} < 0.005$).

4.3 Terra and Aqua MODIS Synergism at local scale

Terra and Aqua MODIS data can be combined in a convenient manner to monitor the local aerosol dynamics in any given location. Figure 10 shows the local (50x50-km) daily mean aerosol optical thickness (AOT) at three wavelengths (470, 550, and 660 nm) from Terra- and Aqua-MODIS over two sites: one in the Eastern US (GSFC) and the other in the Arabian Sea. The data, covering the period of June/July 2002, demonstrate the synergism between the twin sensors, whereby aerosol properties are retrieved from one of the MODIS sensors even when conditions do not allow retrieval from the other.

Since GSFC is also an AERONET site, time series curves of AERONET τ_{a440} and τ_{a670} nm are superimposed on the top panel of Figure 10, which shows that on July 7, when the smoke from the huge Quebec fire reached GSFC, there was no retrieval from Terra-MODIS, perhaps because of cloud cover, but Aqua-MODIS measures the dramatic increase in AOT. *Taubman et al.* [2004] shows a Terra-MODIS image of July 7, with the dense smoke outflow from the Quebec fire reaching GSFC. Although AERONET does not provide level 1.5 or 2.0 AOT over GSFC on July 7, because their automatic cloud filter mistook the dense smoke for clouds, it was

noted that “the τ_{a500} was estimated as ~ 7 (highest ever recorded in AERONET monitoring) from the spectra in the longer wavelengths ($\tau_{a870} \sim 3$)” [Eck *et al.*, 2004, p. 4-2 paragraph 5]. Colarco *et al.* [2004] presented a detailed study of the dynamics of smoke transport from that remarkable Quebec fire event, as well as the effects of the smoke on the local and regional air quality; using satellite, airborne, and ground-based measurements as well as model and trajectory analysis techniques. In particular, Colarco *et al.* [2004] specifically point out the dense smoke outflow from the Quebec fire to GSFC on a July 7 visible image from the SeaWiFS sensor, while the TOMS sensor aerosol retrieval for that date also shows the AOT at 380 nm to be 5 or higher over GSFC.

The bottom panel of Figure 10, representing a remote site over the Arabian Sea, shows where, by coincidence, data points or peaks from Terra- and Aqua-MODIS alternate with one another. This provides for continuity in data, which could have been missed if only one instrument was involved. In both cases, there is beautiful agreement on dates having retrieval from both instruments.

5 CONCLUSIONS

The spectral aerosol optical thickness $\tau_{a\lambda}$ data, produced from Terra-MODIS and Aqua-MODIS from the beginning (2000 and 2002, respectively) up till the end of 2003, have been comprehensively and comparatively evaluated using AERONET data. The data sets evaluated were versions 3 and 4 from Terra-MODIS (T003 and T004) and version 3 from Aqua-MODIS (A003), which was retrieved with almost the same algorithm version as T004. Global assessment of τ_{a550} from T003, T004, and A003, based on quality-assured (level 2.0) AERONET data,

showed that about 67.5%, 55.0%, and 55.5% respectively, fall within the predefined uncertainty range of $\pm(0.05 + 0.2\tau_{a\lambda})$ over land, while about 63.3%, 59.4%, and 62.2%, respectively, fall within the more stringent over-ocean predefined range of $\pm(0.03 + 0.05\tau_{a\lambda})$. For each of the data versions (T003, T004, and A003), the success rate appears to increase with wavelength at least for the evaluated 470 nm to 870 nm wavelength range. Furthermore, as the percentages above show, T003 is slightly more accurate than the later versions (T004 and A003) because these latter versions included retrieval over less than ideal situations such as over brighter surfaces on land. Over land, there is high likelihood of overestimation at low aerosol loading ($\tau_{a550} < 0.20$), with about 55-65% of MODIS $\tau_{a\lambda}$ retrievals falling within the predefined uncertainty bounds. The accuracy improves at moderate loading ($0.20 < \tau_{a550} < 0.70$), with 70% or more of the retrievals at this range falling within the predefined uncertainty envelope. At high aerosol loading ($\tau_{a550} > 0.70$) corresponding to less than 2% of the total retrievals, the accuracy fluctuates erratically. Over ocean, MODIS accuracy is high at low aerosol loading, with over 80% of the retrievals in the range of $\tau_{a550} < 0.05$ falling within the uncertainty envelop. The over-ocean accuracy decreases as the aerosol loading increases. Although the global land and ocean percentages above seem comparable because of the more stringent tolerance over ocean, the respective correlation coefficients and regression slopes and intercepts show that the MODIS over-ocean retrievals are more accurate than over-land products. The main problems identified as influencing the over-land retrieval accuracy relate mainly to background land surface uncertainty due to surface variability, surface brightness, swamps, snow (especially at the melting stage). Other possible influences include scan angle dependence and neglecting to include polarization in the radiative transfer treatment. By contrast, the ocean retrieval, in addition to enjoying the benefit of a smoother dark (ocean) surface, which is favorable to aerosol retrieval (except over

sun glint regions), also benefits from richer information content of the six wavelengths used directly for retrieval (as opposed to only two over land). Overall, the difference in performance between Terra and Aqua is not very significant.

Evaluation of MODIS $\tau_{a\lambda}$ was also conducted at the regional level, to enable the perception of trends of regional performance over time, for easy quantitative application to studies dealing with aerosol distribution and climate forcing. For this aspect of the study, MODIS – AERONET (or M – A) τ_{a550} differences from collocated data were used, such that negative, near-zero, and positive differences would respectively signify underestimation, accurate estimation, and overestimation in the MODIS aerosol retrieval. There were significant regional differences in MODIS quality with respect to AERONET. For the 12 land and 6 ocean regions investigated, those with the most accurate retrievals (with overall average τ_{a550} differences of ± 0.05 or less, with maybe one or two outliers) are: Russia and Brazil (over land), and the Mediterranean, Mid-Atlantic, North-Indian and Central Pacific Oceans (over ocean). The regions with tendency toward underestimation are West Africa and Southern Africa (over land), and Southern Atlantic and Asian Pacific (over ocean). This could be because of inaccurate model assumptions in the parameterization of aerosol spectral properties (e.g. assuming lower absorption than is truly the case with the predominantly highly absorbing southern African savanna smoke [*Ichoku et al.*, 2003], which was rectified early in the algorithm for T004 and A003). Regions with tendency toward overestimation are all over land and include: NW-America, US-Central, US-East, W-Europe, and India (with an overall average overestimation of the order of 0.05), and China, Middle-East, and Australia (with an overall average overestimation of the order of 0.15).

MODIS aerosol spectral optical thickness $\tau_{a\lambda}$ from Terra and Aqua are appreciably accurate over ocean, but have a slightly lower quality over land. However, the data can be used for

various kinds of global, regional, and local studies with acceptable accuracy. Analysis of MODIS $\tau_{a\lambda}$ subdivided into three size ranges based on different AERONET Ångström exponent ranges ($\alpha < 0.7$, $0.7 < \alpha < 1.8$, and $\alpha > 1.8$, respectively representing large, midrange, and small size modes), shows that the $\tau_{a\lambda}$ values are more accurate over ocean than over land. Time series of the group monthly averages of data acquired over AERONET sites, both from Terra-MODIS and AERONET, show a net steady increase in the average loading of the large size mode ($\alpha < 0.7$) from 2000 to 2003, especially over ocean. MODIS regional monthly average τ_{a550} time series (based on full spatial sampling) show large variations in seasonal cycles between regions, but do not show a net increase of aerosol loading even over dust-dominated regions. There is great resemblance in the cyclic amplitude and phase between regions with common aerosol type, source, or distribution characteristics. Analysis of the regional daily mean τ_{a550} differences between Terra and Aqua for the various study regions show that, although there are daily differences between the morning and afternoon observations from the twin sensors in most regions, the magnitudes of which vary from region to region, none of the regions shows any consistent morning-to-afternoon increase or decrease in aerosol loading. Combined plots of the Terra-MODIS and Aqua-MODIS $\tau_{a\lambda}$ at the local scale for an over-land urban and an over-ocean dust environments, both of which contained some smoke, show that Terra and Aqua observations can provide for data continuity at different temporal scales.

Finally, the evaluation done in this study has been extensive, employing an unprecedented number of collocated MODIS/AERONET data point pairs: over 23,000 for Terra and over 10,000 for Aqua. Although MODIS $\tau_{a\lambda}$ accuracies do not reach AERONET accuracy levels (of 0.02), especially over land, given that MODIS is the first sensor used for operational aerosol retrieval at moderate scale both over land and ocean, and considering the numerous problems

posed to aerosol retrieval by the surface background, especially over land, and the potential sampling mismatch in comparing averages from MODIS spatially variable data space and AERONET temporally variable data space, the overall performance of the Terra and Aqua twin MODIS sensors in aerosol retrieval is excellent. Nevertheless, the MODIS aerosol team continues to evaluate and understand the sources of uncertainty and continues to develop and implement strategies aimed at systematically eliminating as much uncertainties as possible in order to generate top quality products for all types of applications.

Acknowledgement

This study was conducted as part of the MODIS aerosol retrieval and validation project, supported under the NASA Earth Observing System (EOS) program under the direction of Michael King. We would like to thank the various MODIS atmosphere software development and support teams for the production and distribution of the MODIS data, particularly the aerosol group led by Yoram Kaufman, who together with Didier Tanré, formulated the MODIS aerosol algorithms. We are also very grateful to Yoram Kaufman for very helpful ideas and comments on this paper. We thank the AERONET PIs and team members for collecting, processing, and making available ground-based aerosol observations around the world. Special thanks go to Brent Holben (AERONET PI), for authorizing the use of the AERONET data, and to Ilya Slutsker and David Giles for maintaining the AERONET data system and web site and for compiling the data needed for MODIS validation. Indeed, the AERONET project has been very instrumental to the success of the validation of MODIS aerosol products, and much credit is due to those who conceived the idea of AERONET.

REFERENCES

- Christopher, S. A., and J. Zhang, Shortwave Aerosol Radiative Forcing from MODIS and CERES observations over the oceans, *Geophys. Res. Lett.*, **29**(18), 1859, doi:10.1029/2002GL014803, 2002.
- Chu, D. A., Y. J. Kaufman, C. Ichoku, L. A. Remer, D. Tanré, and B. N Holben, Validation of MODIS aerosol optical depth retrieval over land., *Geophys. Res. Lett.*, **29**, **10.1029/2001GL013205**, 2002.
- Chu, D. A., Y. J. Kaufman, G. Zibordi, J. D. Chern, J. Mao, C. Li, and B. N. Holben, Global monitoring of air pollution over land from the Earth Observing System-Terra moderate resolution imaging spectroradiometer (MODIS), *J. Geophys. Res.*, **108**, **10.1029/2002JD003179**, 2003.
- Colarco, P. R., M. R. Schoeberl, B. G. Doddridge, L. T. Marufu, O. Torres, and E. J. Welton (2004), Transport of smoke from Canadian forest fires to the surface near Washington, D.C.: Injection height, entrainment, and optical properties, *J. Geophys. Res.*, **109**, D06203, doi:10.1029/2003JD004248.
- Dubovik, O., B. N. Holben, T. F. Eck, A. Smirnov, Y. J. Kaufman, M. D. King, D. Tanré and I. Slutsker, Variability of absorption and optical properties of key aerosol types observed in worldwide locations. *J. Atmos. Sci.*, **59**, 590-608, 2002.
- Eck, T. F., B. N. Holben, J. S. Reid, O. Dubovik, A. Smirnov, N. T. O'Neill, I. Slutsker, and S. Kinne, Wavelength dependence of the optical depth of biomass burning, urban, and desert dust aerosols, *J. Geophys. Res.*, **104**, 31,333-31,349, 1999.
- Eck, T. F., B. N. Holben, J. S. Reid, N. T. O'Neill, J. S. Schafer, O. Dubovik, A. Smirnov, M. A. Yamasoe, and P. Artaxo, High aerosol optical depth biomass burning events: A

- comparison of optical properties for different source regions, *Geophys. Res. Lett.*, 30(20), 2035, doi:10.1029/2003GL017861, 2003.
- Gao, B.-C., Y. J. Kaufman, D. Tanré, and R.-R. Li, Distinguishing tropospheric aerosols from thin cirrus clouds for improved aerosol retrievals using the ratio of 1.38- μ m and 1.24- μ m channels, *Geophys. Res. Lett.*, **29**, 10.1029/2002GL015475, 2002.
- Holben, B. N., T. F. Eck, I. Slutsker, D. Tanré, J. P. Buis, A. Setzer, E. Vermote, J. A. Reagan, Y. J. Kaufman, T. Nakajima, F. Lavenu, I. Jankowiak and A. Smirnov, AERONET--A federated instrument network and data archive for aerosol characterization, *Rem. Sens. Environ.*, **66**, 1-16, 1998.
- Holben, B. N., D. Tanré, A. Smirnov, T. F. Eck, I. Slutsker, N. Abuhassan, W. W. Newcomb, J. S. Schafer, B. Chatenet, F. Lavenu, Y. J. Kaufman, J. Vande Castle, A. Setzer, B. Markham, D. Clark, R. Frouin, R. Halthore, A. Karnieli, N. T. O'Neill, C. Pietras, R. T. Pinker, K. Voss, and, G. Zibordi, An emerging ground-based aerosol climatology: aerosol optical depth from AERONET, *J. Geophys. Res.*, **106**, 12,067-12,097, 2001.
- Ichoku, C., D. A. Chu, S. Mattoo, Y. J. Kaufman, L. A. Remer, D. Tanré, I. Slutsker, and B. Holben, A spatio-temporal approach for global validation and analysis of MODIS aerosol products. *Geophys. Res. Lett.*, **29**, 10.1029/2001GL013206, 2002.
- Ichoku, C., L. A. Remer, Y. J. Kaufman, R. Levy, D. A. Chu, D. Tanré, and B. Holben, MODIS Observation of Aerosols and Estimation of Aerosol Radiative Forcing Over Southern Africa during SAFARI 2000, *J. Geophys. Res.*, **108**, 10.1029/2002JD002366, 2003.
- Ichoku, C., Y. J. Kaufman, L. A. Remer, and R. Levy, Global aerosol remote sensing from MODIS, *Adv. Space Res.*, in press, 2004.

- Kaufman, Y. J., B. N. Holben, D. Tanré, I. Slutsker, A. Smirnov, and T. F. Eck, Will aerosol measurements from Terra and Aqua polar orbiting satellites represent the daily aerosol abundance and properties, *Geophys. Res. Letters*, **27**, 3861-3864, 2000.
- Kaufman, Y. J., D. Tanré, L. A. Remer, E. F. Vermote, A. Chu, and B. N. Holben, Operational remote sensing of tropospheric aerosol over land from EOS moderate resolution imaging spectroradiometer, *J. Geophys. Res.*, **102**, 17,051-17,067, 1997.
- Kaufman, Y. J., D. Tanré, and O. Boucher, A satellite view of aerosols in the climate system, *Nature*, **419**, 215-223, 2002.
- Koren, I., Kaufman, Y. J., L. A. Remer, and J. V. Martins, Measurement of the effect of Amazon smoke on inhibition of cloud formation, *Science*, **303**, 1342-1345, 2004.
- Levy, R. C., L. A. Remer, and Y. J. Kaufman, How does the omission of polarization affect the MODIS aerosol retrieval over land?, *IEEE Trans. Geosci. Remote Sens.*, submitted, 2004.
- Levy, R. C., L. A. Remer, D. Tanre, Y. J. Kaufman, C. Ichoku, B. N. Holben, J. Livingston, P. Russell, and H. Maring, Evaluation of the MODIS retrievals of dust aerosol over the ocean during PRIDE, *J. Geophys. Res.*, **108**, 10.1029/2002JD002460, 2003.
- Lyapustin, A. I. and Y. J. Kaufman, Role of adjacency effect in the remote sensing of aerosol, *J. Geophys. Res.*, **106**, 11,909-11,916, 2001.
- Martins, J. V., D. Tanré, L. Remer, Y. Kaufman, S. Mattoo, R. Levy, MODIS cloud screening for remote sensing of aerosols over oceans using spatial variability, *Geophys Res Lett.*, **29**, 10.1029/2001GL013252, 2002.
- Remer, L. A., Y. J. Kaufman, D. Tanré, S. Mattoo, D. A. Chu, J. V. Martins, R.-R. Li, C. Ichoku, R. Levy, R. G. Kleidman, T. F. Eck, E. Vermote, and B. N. Holben, The MODIS aerosol algorithm, products and validation, *J. Atmos. Sci.*, in press, 2004.

- Remer, L. A., D. Tanré, Y. J. Kaufman, C. Ichoku, S. Mattoo, R. Levy, D. A. Chu, B. N. Holben, O. Dubovik, Z. Ahmad, A. Smirnov, J. V. Martins, and R.-R. Li, Validation of MODIS Aerosol Retrieval Over Ocean, *Geophys. Res. Lett.*, **29**, 10.1029/2001GL013204, 2002.
- Smirnov, A., B.N. Holben, T.F. Eck, O. Dubovik, and I. Slutsker, Cloud screening and quality control algorithms for the AERONET data base, *Remote Sens. Environ.*, **73**, 337-349, 2000.
- Smirnov, A., B. N. Holben, T. F. Eck, I. Slutsker, B. Chatenet, and R. T. Pinker, Diurnal variability of aerosol optical depth observed at AERONET (Aerosol Robotic Network) sites, *Geophys. Res. Lett.*, **29** (23), 2115, doi:10.1029/2002GL016305, 2002.
- Tanré, D., Y. J. Kaufman, M. Herman, and S. Mattoo, Remote sensing of aerosol properties over oceans using the MODIS/EOS spectral radiances, *J. Geophys. Res.*, **102**, 16971-16988, 1997.
- Taubman, B. F., L. T. Marufu, B. L. Vant-Hull, C. A. Piety, B. G. Doddridge, R. R. Dickerson, and Z. Li (2004), Smoke over haze: Aircraft observations of chemical and optical properties and the effects on heating rates and stability, *J. Geophys. Res.*, **109**, D02206, doi:10.1029/2003JD003898.
- Yu, H., R. E. Dickinson, M. Chin, Y. J. Kaufman, B. N. Holben, I. V. Geogdzhayev, and M. I. Mishchenko, Annual cycle of global distributions of aerosol optical depth from integration of MODIS retrievals and GOCART model simulations, *J. Geophys. Res.*, **108**(D3), 4128, doi:10.1029/2002JD002717, 2003.

Figure Captions

Figure 1: Multi-year (2000 – 2003) average aerosol optical thickness (AOT) at 550 nm wavelength from Terra-MODIS showing rectangular boundaries of various regions referenced in this study. Land regions are delimited by solid lines with numeric labels (1 – 12), while ocean regions are delimited by dotted lines with alphabetic labels (A – F). Since MODIS currently does not retrieve aerosols over highly bright surfaces such as Greenland, the Sahara, and the Antarctica, the purple patches (zero values) in those regions may be due to artifacts from the plotting software.

Figure 2: Modified scatter plots of MODIS global class average AOT (based on collocated AERONET AOT bins) against the AERONET AOT bin center values, for T003, T004, and A003 over land (at 470, 550, 660 nm wavelengths) and ocean (at 550, 660, 870 nm wavelengths). The standard deviations of the AOT classes for MODIS are shown as error bars only for the 550 nm curves (to limit clutter). The dotted diagonal line is the 1-to-1 line, while the pair of near diagonal broken lines are the bounds of the uncertainty envelops. The total number of data points (np) used in each data group is shown on each panel, while the cumulative counts of data points in each class are plotted at all wavelengths represented. The percent proportion of MODIS AOT at 550 nm falling within the specified uncertainty bounds in each class are plotted ($\%pass_{550}$).

Figure 3a: (Western Hemisphere) time series of regional monthly mean AOT at 550 nm and corresponding (MODIS – AERONET) differences for the different MODIS aerosol data versions (T003, T004, and A003).

Figure 3b: (Eastern Hemisphere) time series of regional monthly mean AOT at 550 nm and corresponding (MODIS – AERONET) differences for the different MODIS aerosol data versions (T003, T004, and A003).

Figure 4: Summary of regional comparison of MODIS AOT at 550 nm with AERONET level 1.5 AOT. The bars represent the overall regional averages computed from the MODIS 50x50 km local averages over AERONET stations for the entire period of each data set (T003, T004, or A003). The topping spikes are the corresponding average MODIS-AERONET differences, and represent MODIS overestimation or underestimation with respect to AERONET depending on whether they project above or below the top of the bar.

Figure 5: Plots of global mean (MODIS – AERONET) differences of AOT at 550 nm, grouped according to sensor zenith angle bins (5-deg intervals), for different Terra and Aqua MODIS data versions (T003, T004, and A003) over land (thin lines) and ocean (thick lines), plotted against their respective sensor zenith angle bins. Error bars (shown only for the land and ocean T004, to limit clutter) are the corresponding standard deviations.

Figure 6: Spectral plots of the three-year (2000-2003) overall average aerosol optical thickness (AOT) from MODIS and AERONET, computed from collocated local averages (MODIS: 50x50 km, AERONET: +30 min), partitioned according to three AERONET

Ångstrom exponent ranges ($A_{exp} < 0.7$, $0.7 < A_{exp} < 1.8$, or $A_{exp} > 1.8$). The plots are shown separately (a – d) and combined (e) for Terra and Aqua overpass times over land and ocean.

Figure 7: Monthly mean aerosol optical thickness (AOT) from MODIS and AERONET for the overpass times of Terra and Aqua over land and ocean. The averages were computed from local means (MODIS: 50x50 km; AERONET: ± 30 min) over all AERONET stations grouped according to three ranges of AERONET Ångstrom exponent ($\alpha < 0.7$, $0.7 < \alpha < 1.8$, or $\alpha > 1.8$).

Figure 8: Time series of regional monthly average AOT at 550 nm, derived directly from MODIS level 2 (10-km resolution) daily aerosol products. The regions are grouped as western hemisphere WH land (top panel), eastern hemisphere EH land (middle panel), and ocean (bottom panel). Note that the scale of the ocean panel is twice that of the land plots.

Figure 9a: (Western Hemisphere) time series of regional daily average Terra-MODIS AOT at 550 nm (lower points, left scale) co-plotted with the corresponding (Aqua – Terra) τ_{a550} differences (upper points, right scale). The regional averages were derived directly from MODIS level 2 (10-km resolution) aerosol data from Terra and Aqua before the (Aqua – Terra) τ_{a550} daily differences $D^{A-T} \tau_{a550}$ were calculated.

Figure 9b: (Eastern Hemisphere) time series of regional daily average Terra-MODIS AOT at 550 nm (lower points, left scale) co-plotted with the corresponding (Aqua – Terra) τ_{a550} differences (upper points, right scale). The regional averages were derived directly from MODIS level 2 (10-km resolution) aerosol data from Terra and Aqua before the (Aqua – Terra) τ_{a550} daily differences $D^{A-T} \tau_{a550}$ were calculated.

Figure 10: Local (50x50-km) daily mean Terra- and Aqua-MODIS aerosol optical thickness (AOT) at three wavelengths (470, 550, and 660 nm) over two sites (one in the Eastern US (GSFC) and the other in the Arabian Sea) in June/July 2002. Terra data are represented by thin solid lines and filled symbols, while Aqua data are represented by dotted lines and open symbols. AERONET mean AOT at 440 and 670 nm wavelengths (averaged within ± 30 -min of Terra or Aqua overpass) are superimposed on the GSFC panel (thick solid curves), since this is also an AERONET site, to demonstrate that MODIS (on Terra and Aqua) observed the same pattern of time series as the AERONET ground-based measurements.

Table Captions

Table 1: Regions selected for this study, as shown in Figure 1, with corresponding boundary coordinates and dominant aerosol types.

Table 2a: Over-land AERONET sites where MODIS shows less than 50% rate of falling within error bounds and probable causes. A question mark (?) in the probable cause column indicates 'not known'. There were a total of 175 land AERONET sites involved in this study. Sites indicated with an X in the first column are completely excluded from MODIS validation analysis because of known site-specific problems not related to MODIS retrieval.

Table 2b: Over-ocean AERONET sites where MODIS shows less than 50% rate of falling within error bounds and probable causes. A question mark (?) in the probable cause column indicates 'not known'. There were a total of 56 ocean AERONET sites involved in this study. Sites indicated with an X in the first column are completely excluded from MODIS validation analysis because of known site-specific problems not related to MODIS retrieval.

Table 3: Parameters of the global accuracy ratio (*%pass*) and linear regression fit of 50x50-km average MODIS level 2 AOT against ± 30 -min average AERONET levels 1.5 and 2.0 AOT.

Table 4a: Summary of the regional validation of MODIS AOT with AERONET over land.

Table 4b: Summary of the regional validation of MODIS AOT with AERONET over ocean.

Table 5: Average regional (Aqua - Terra) difference of AOT at 550 nm for the period of June 2002 to December 2003.

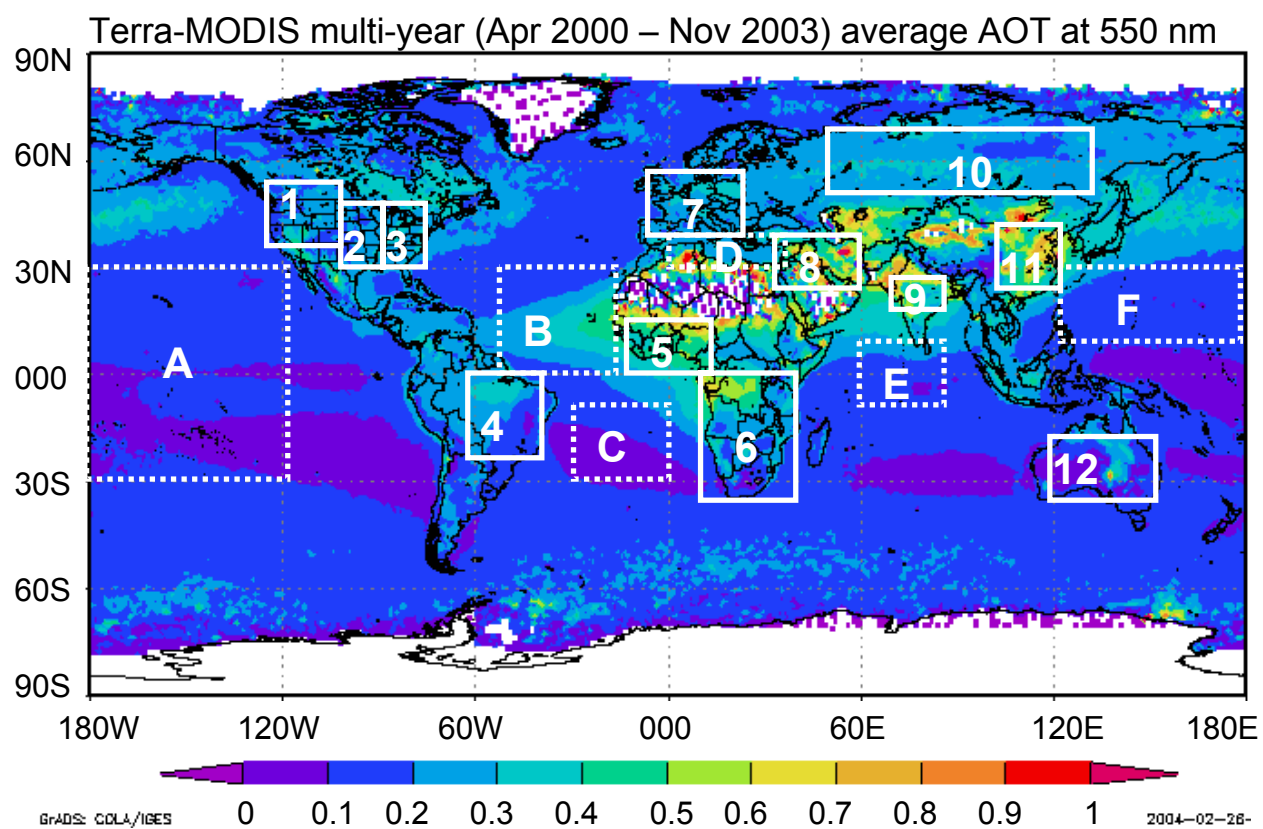


Figure 1

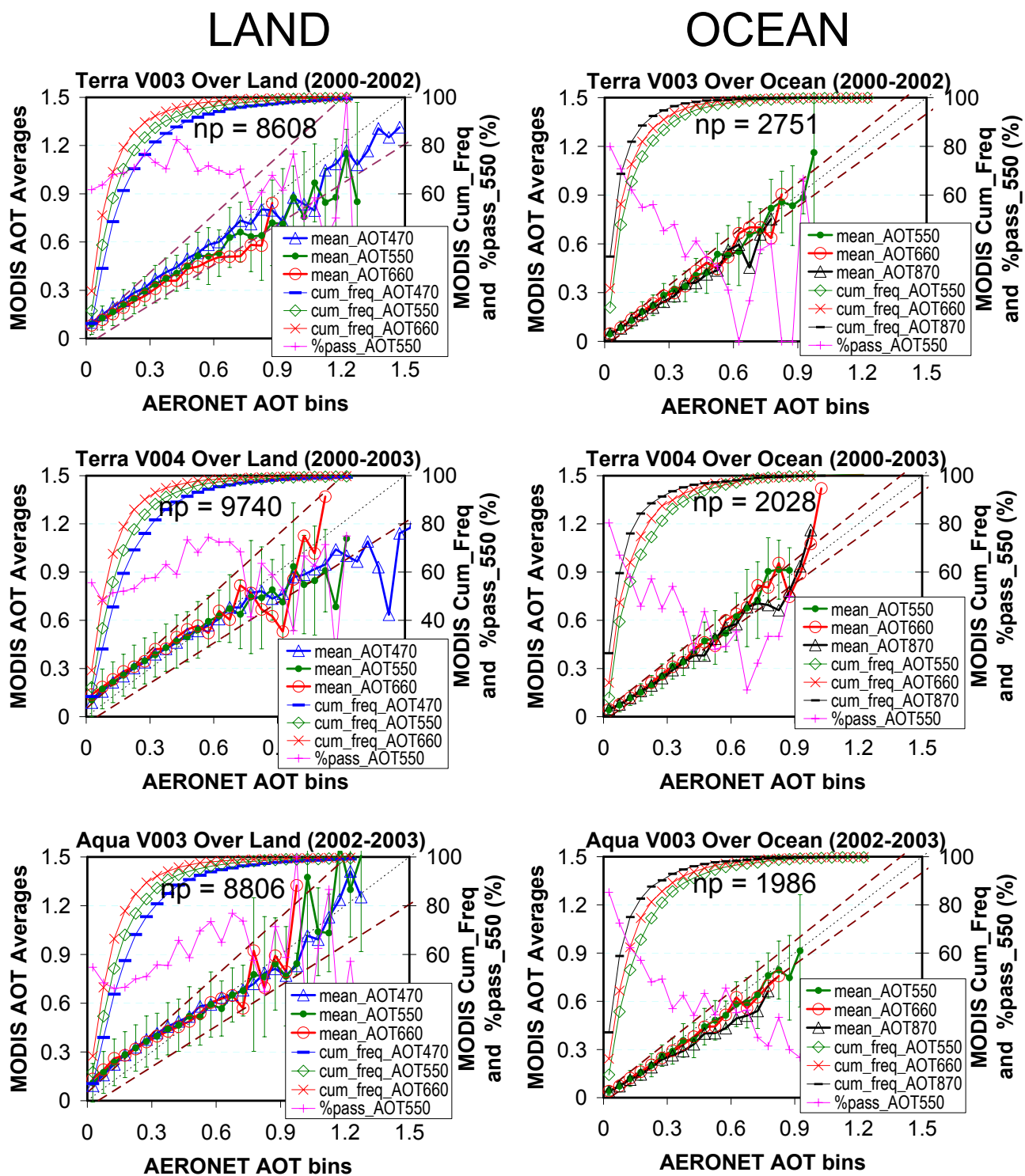


Figure 2

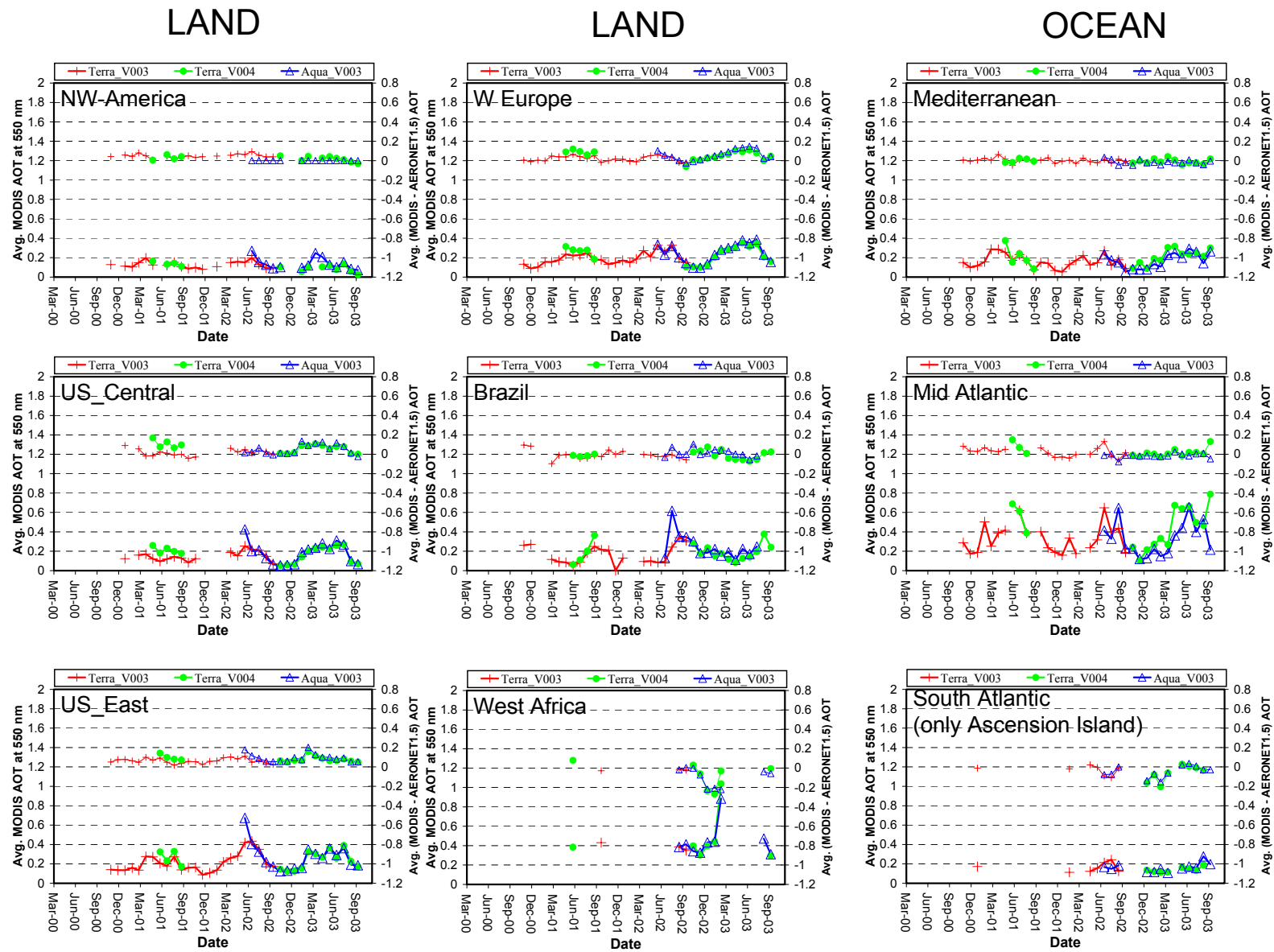


Figure 3a

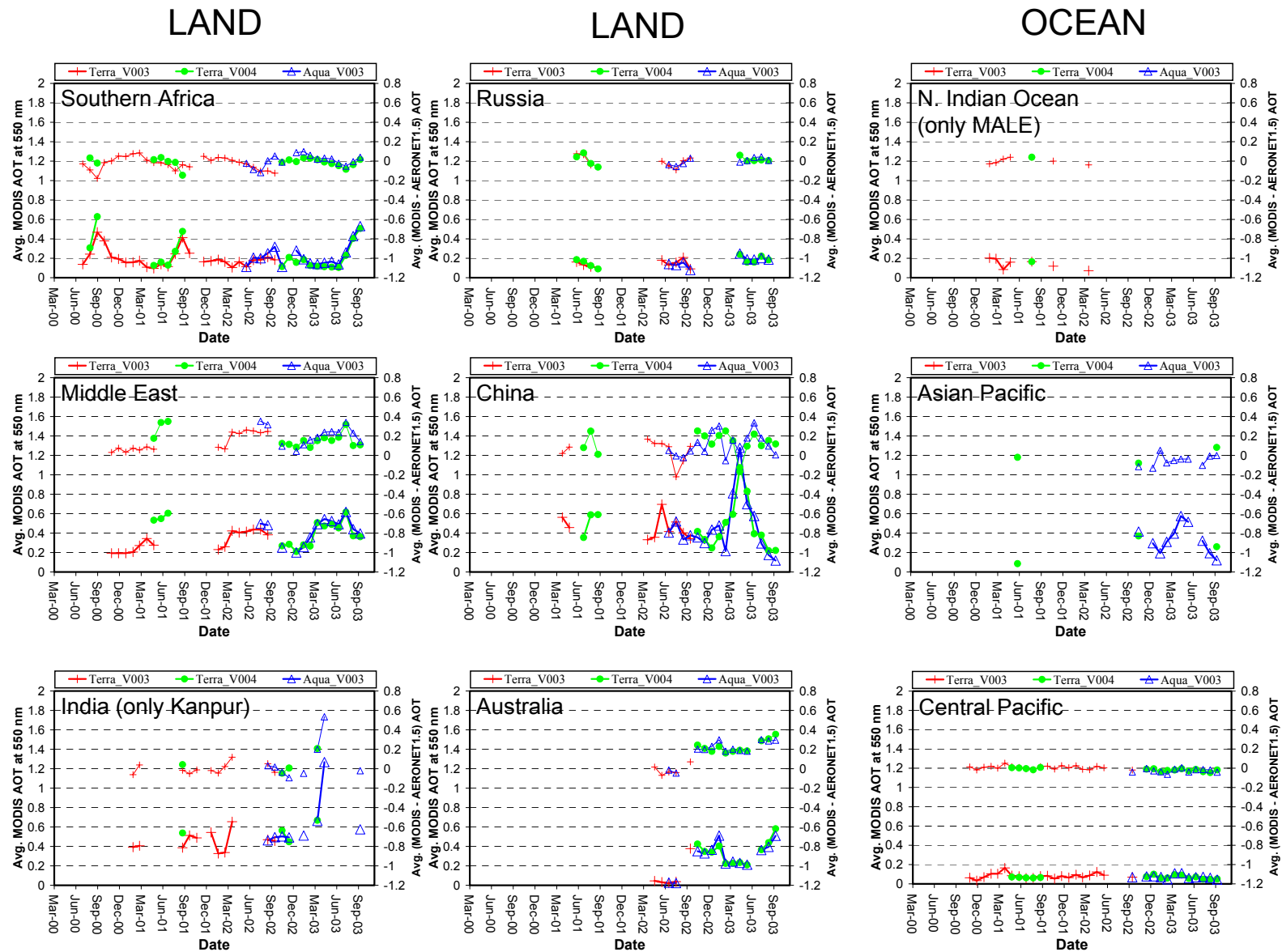


Figure 3b

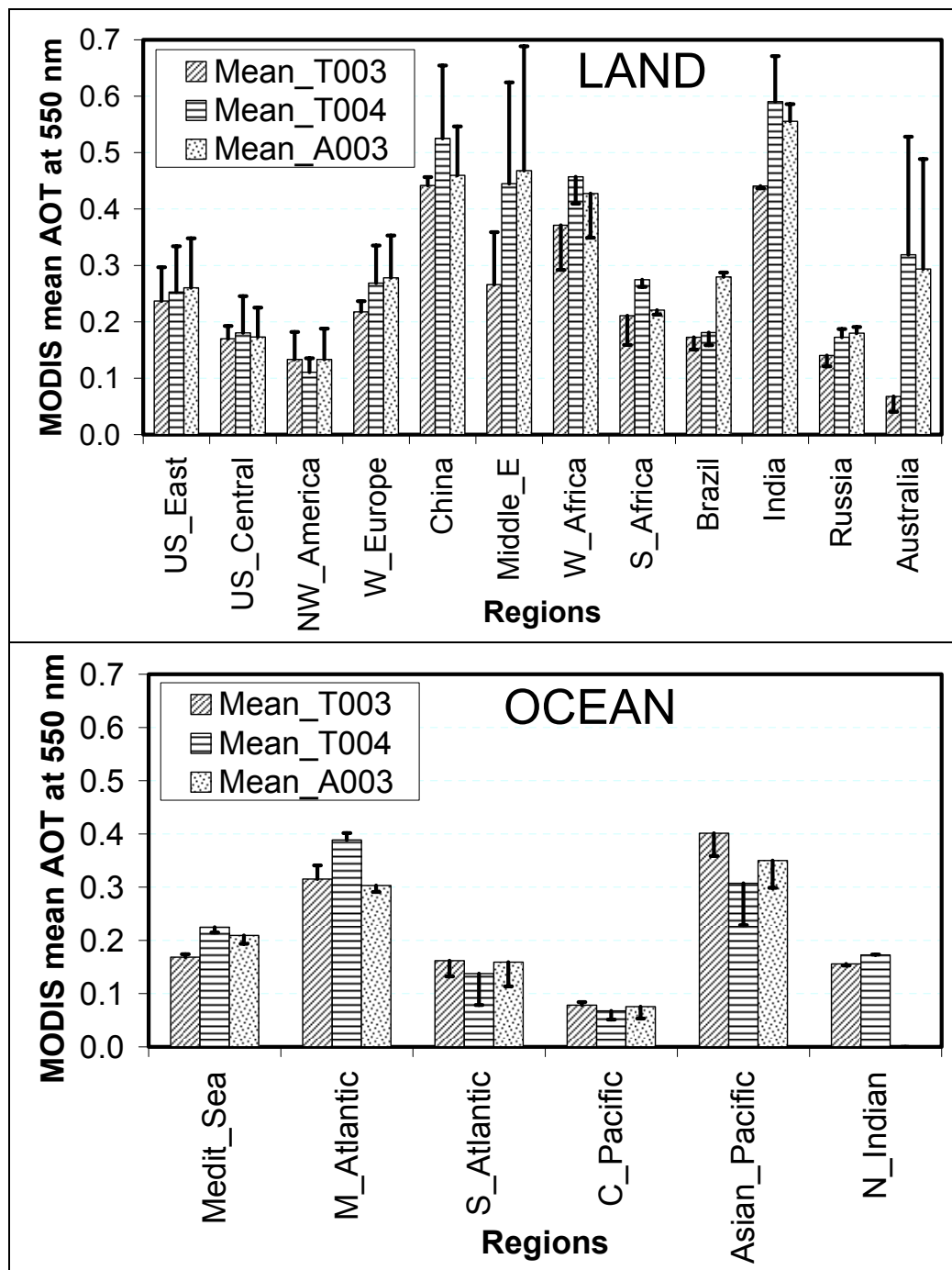


Figure 4

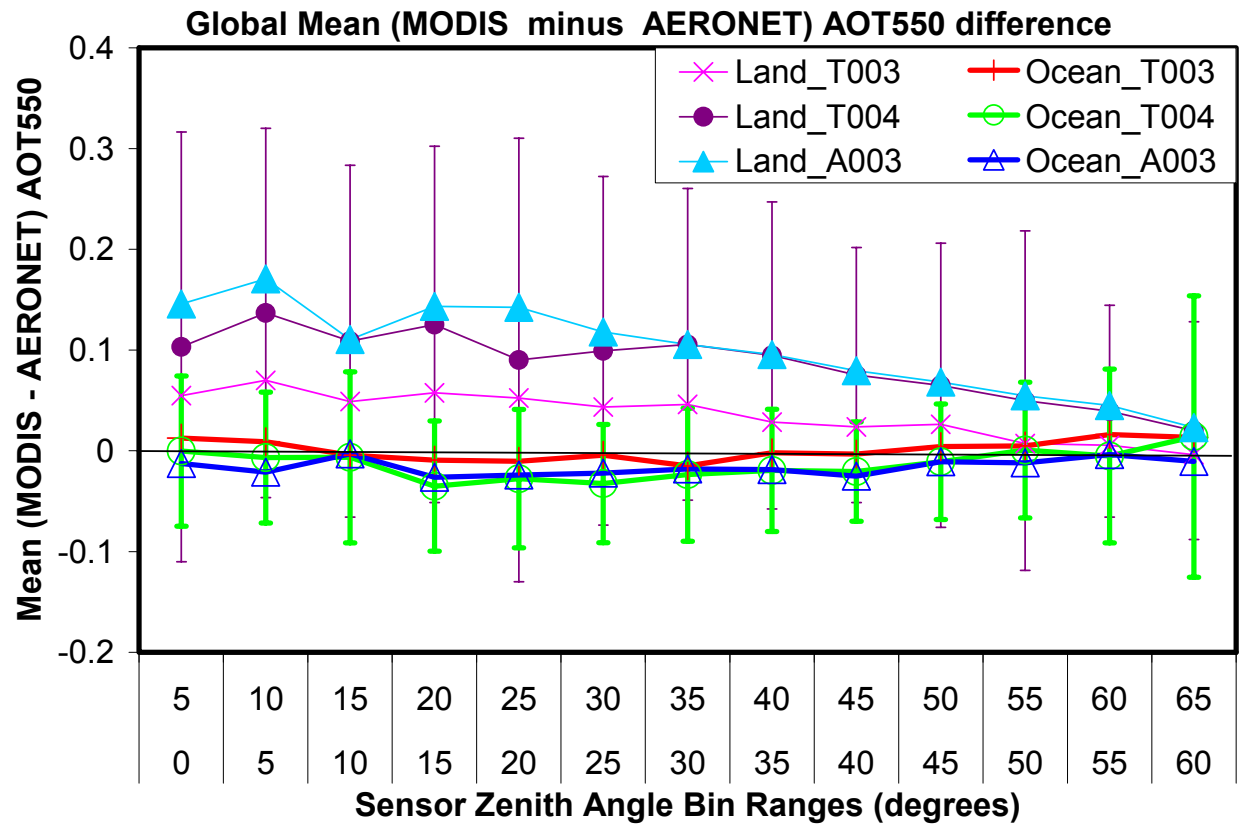


Figure 5

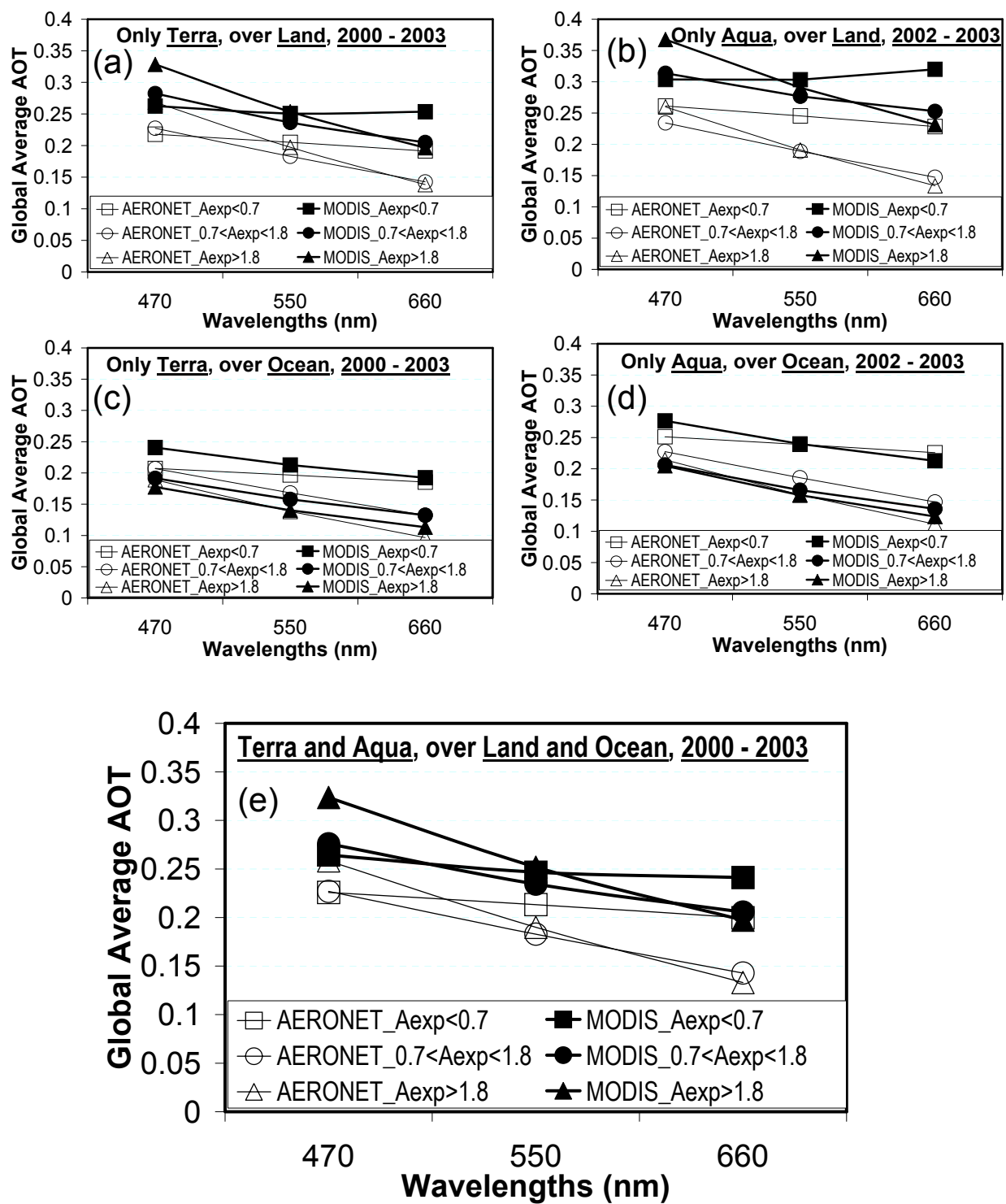


Figure 6

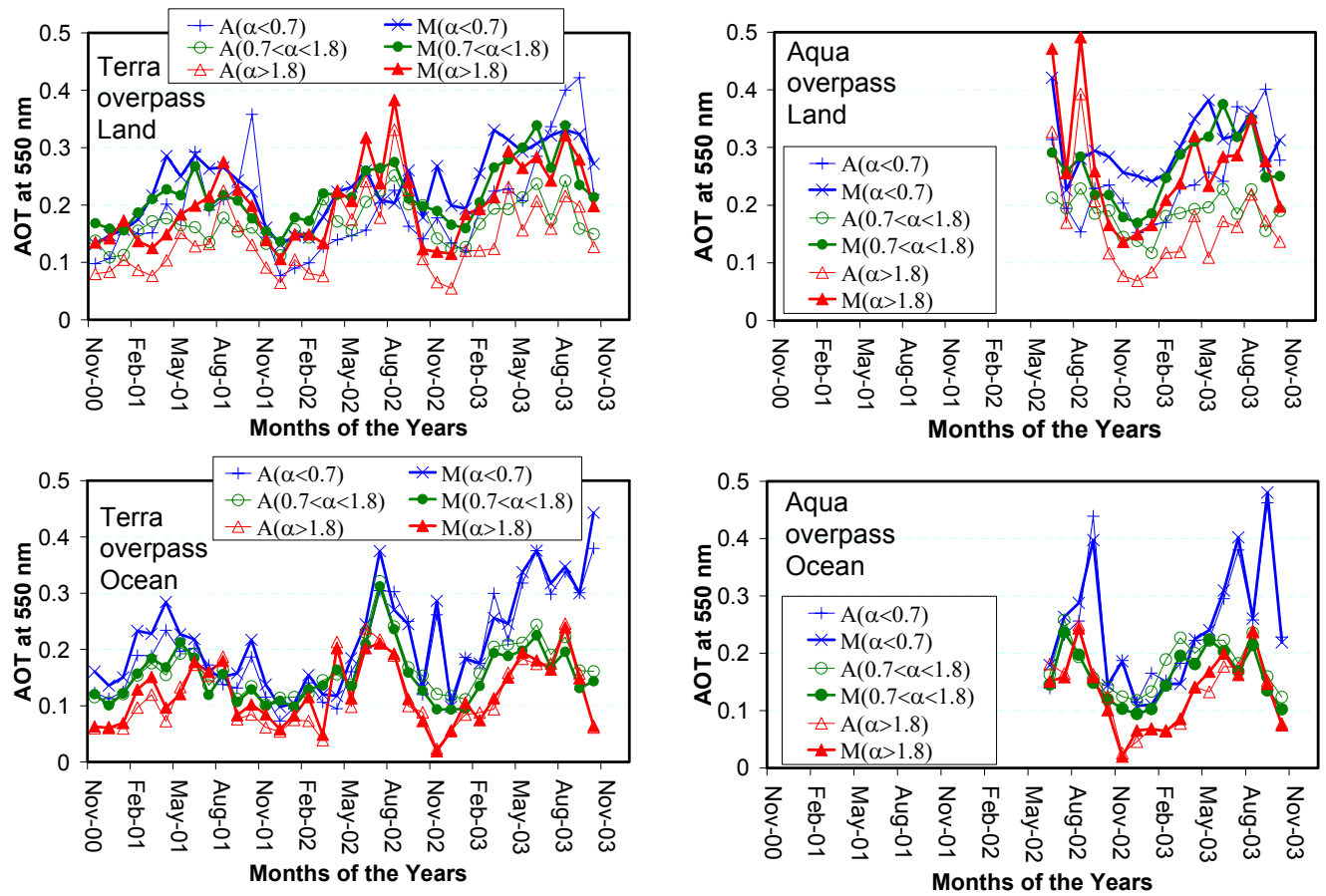


Figure 7

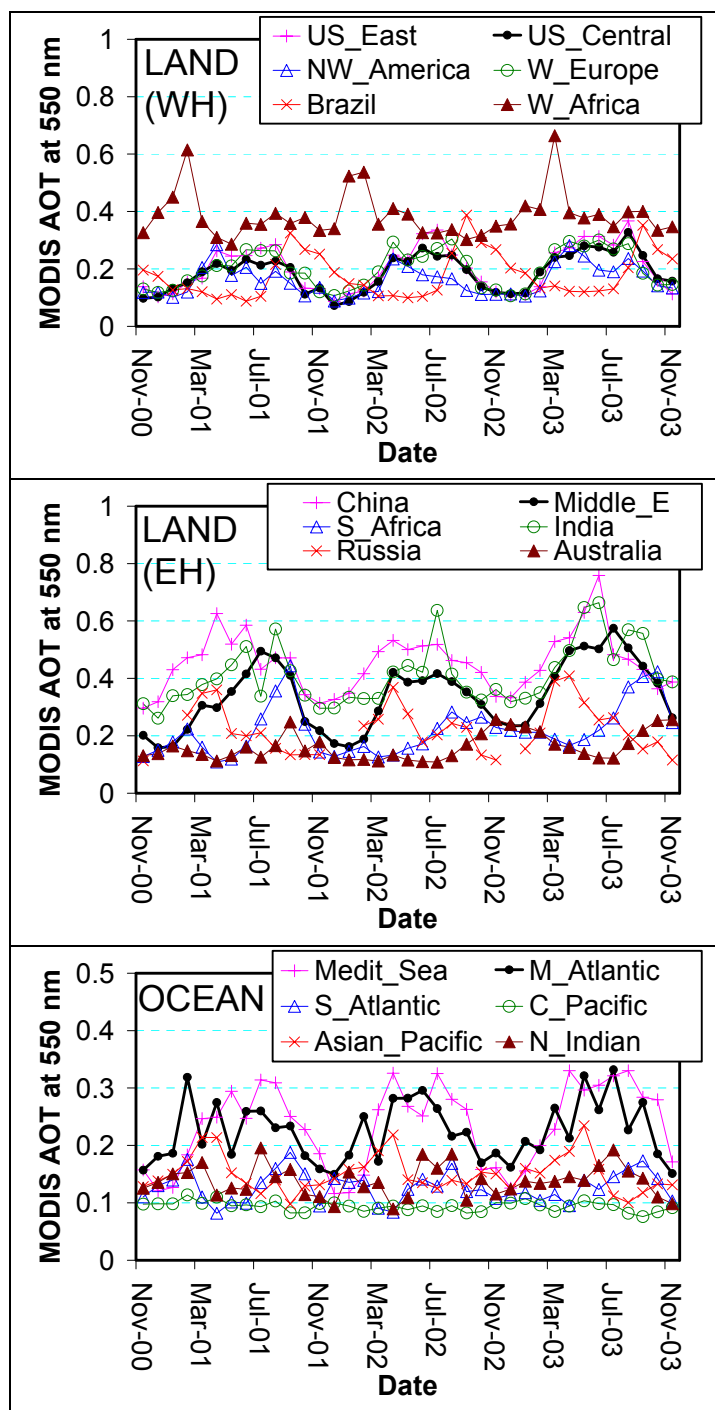


Figure 8

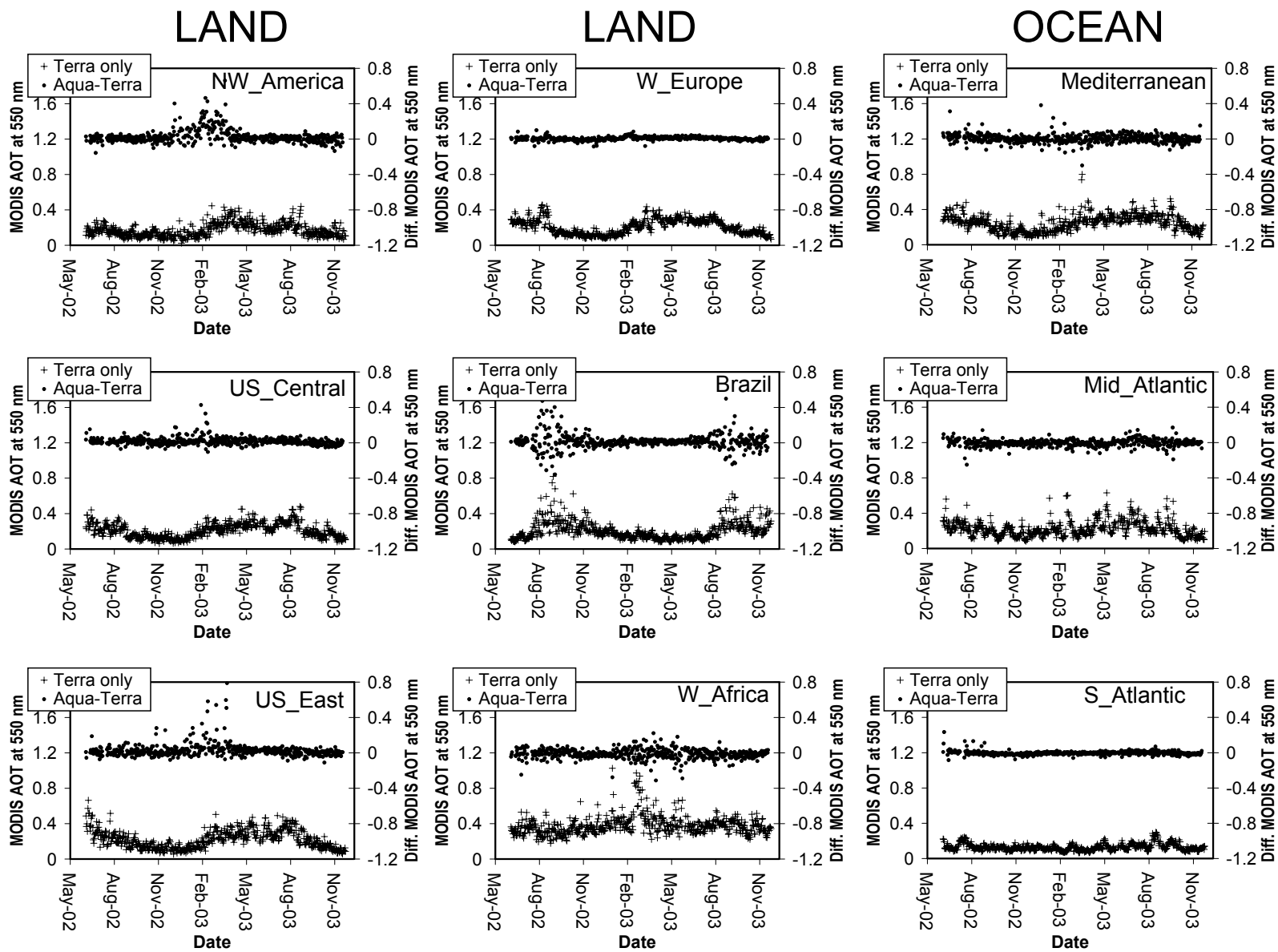


Figure 9a

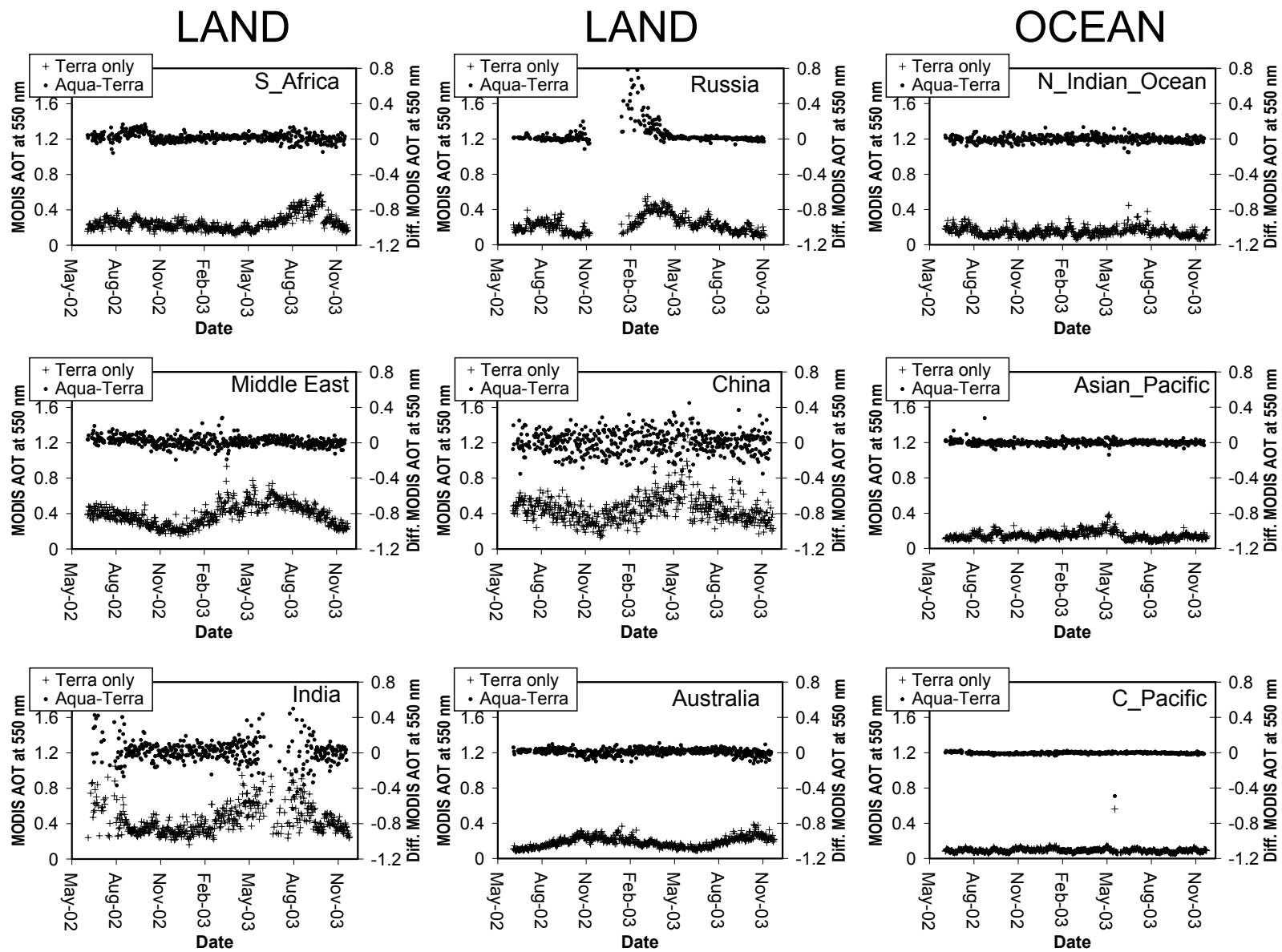


Figure 9b

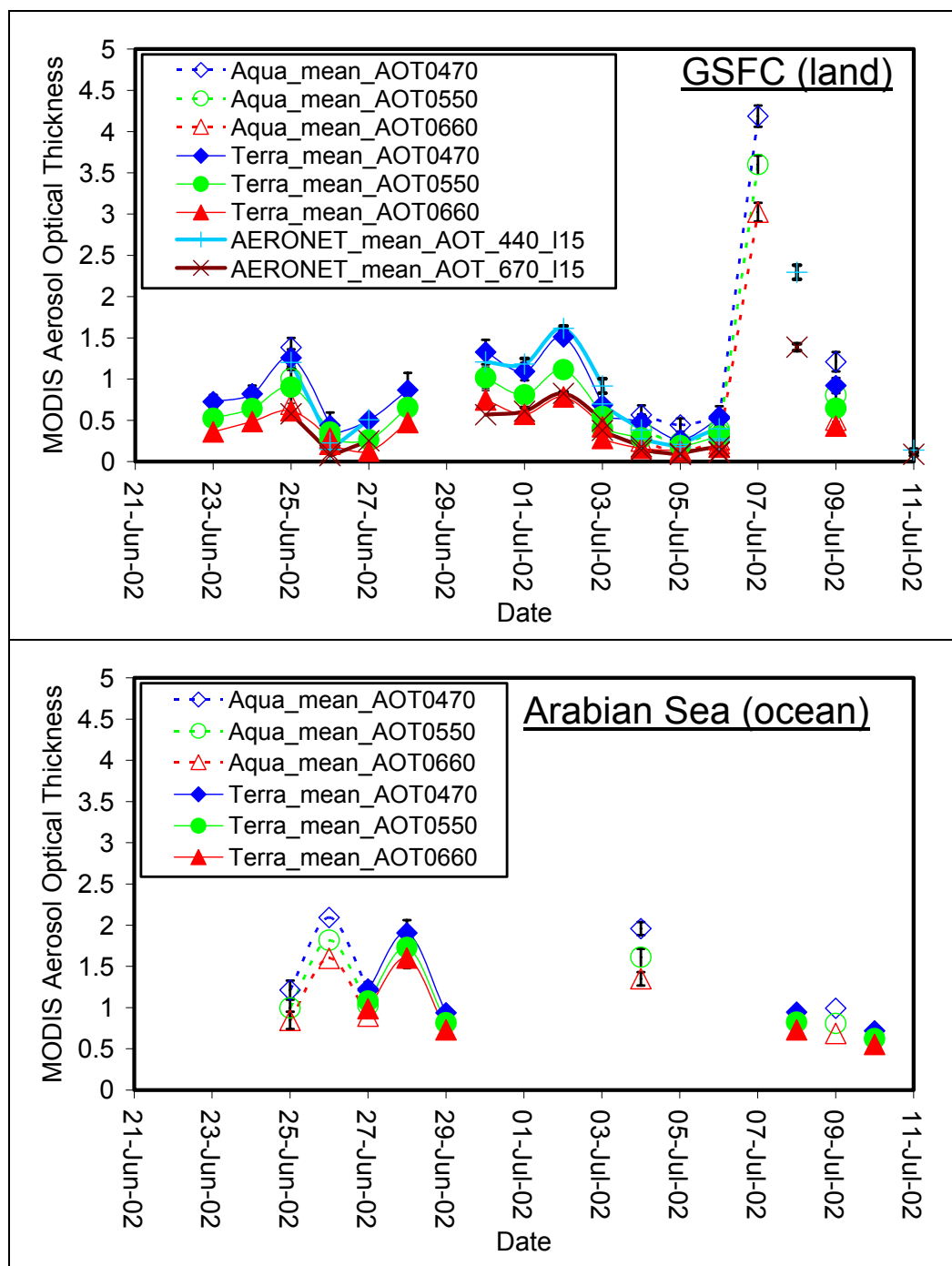


Figure 10

Table 1: Regions selected for this study, as shown in Figure 1, with corresponding boundary coordinates and dominant aerosol types.

Label	Name	Min_Lon	Max_Lon	Min_Lat	Max_Lat	Aerosol_Type
LAND						
1	NW_America	-125	-110	40	60	smoke
2	US_Central	-110	-90	30	50	mixed
3	US_East	-90	-70	30	50	Urban/industrial pollution
4	Brazil	-60	-40	-25	0	smoke
5	W_Africa	-15	15	0	15	mixed
6	S_Africa	10	40	-35	0	smoke (some dust, urban/ind)
7	W_Europe	-10	30	40	60	Urban/industrial pollution
8	Middle_E	30	60	20	40	dust
9	India	70	85	20	30	mixed
10	Russia	50	140	50	70	smoke
11	China	100	120	25	45	mixed
12	Australia	120	150	-35	-15	mixed
OCEAN						
A	C_Pacific	-180	-120	-30	30	oceanic
B	M_Atlantic	-50	-15	0	30	dust/smoke
C	S_Atlantic	-30	10	-30	0	smoke (some dust)
D	Medit_Sea	0	35	30	40	mixed
E	N_Indian	60	90	-10	10	pollution/dust
F	Asian_Pacific	120	180	0	40	mixed

Table 2a

Excluded	Name	ndata	%pass	Probable cause(s) of elevated uncertainty
LAND				
	Arica	9	0	Urban site, bordering on the Atacama desert. Extremely arid.
	Bac Lieu	8	0	Swampy river delta (0% pass over ocean).
	Barrow	16	13	Snow and melting snow problem.
	Beijing	69	39	Urban surface variability. Mixed aerosol types.
	Bratts Lake	74	16	Prairie. Glacial terrain. Dotted by pothole lakes.
	Brookhaven	43	35	On New York Long Island: some water, and sandy beaches.
	Carpentras	126	46	Located in the foothills of mountains.
	CCNY	60	32	New York City urban surface variability.
	CEILAP-BA	94	36	Buenos Aires urban surface variability. Nearness to wide river delta.
	Chen-Kung Univ	7	38	Uncertainty in data sampling. Urban with adjacent mountains.
	Chulalongkorn	7	31	Bangkok, Thailand urban surface variability. Instrument on high rise building.
	Churchill	13	0	Tundra vegetation, snow, ice.
	Coconut Island	24	29	Island site with mountains nearby, cloudy.
	Coleambally	40	48	Arid area of Australia.
	Corcoran	83	38	Site in the irrigated central valley of California, with nearby lakes.
X	COVE	57	20	Offshore platform. Only limited land strip: swampy or sandy.
X	CRYSTAL FACE	1	0	Coastal Florida with swamps and sandy beaches.
X	Dhabi	1	0	Very arid coastal site.
	Dunkerque	30	37	Coastal site and urban surface variability.
	El Arenosillo	211	25	Sandy soil with pine trees, nearby marshes.
	ETNA	9	22	AERONET instrument on slope of high mountain, not total column aerosol.
	Etosha Pan	10	37	Extremely arid and bright salt pan.
	Evora	56	16	?
	FORTH CRETE	134	20	Semi-arid.
	Fresno	117	47	Located in a region with irrigated agricultural valleys and mountains.
	GISS	68	39	New York City urban surface variability.
	Gotland	120	44	Snow and melting snow problem. Coastal.
	Guadeloup	11	16	Suspected AERONET instrument problem (some time periods).
	Halifax	79	34	Snow and melting snow problem. Coastal harbor, with possible floating ice.
X	Helgoland	5	31	North Sea offshore platform, nearby land is small and rocky island. Ice, snow, melting snow.
X	Ilorin	35	33	Known AERONET instrument problem (Apr 25 - Aug 30, 2003).
	ISDGM_CNR	129	21	Venise urban surface variability, water canals.
X	Kejimikujik	11	26	AERONET instrument problem, clouds.
	La Jolla	69	35	Urban and sandy beach.
	Lake Argyle	77	3	Semi-arid, station near lake.
	Lanai	69	30	Island surrounded by ocean. Limited land surface, which is semi-arid.
	Longyearbyen	20	33	Very high latitude. Ice, sea ice, Snow, and melting snow problem.
	Maricopa	144	6	Site in irrigated fields adjacent to arid bright surfaces.
X	Mauna Loa	136	43	High altitude (~3.4 km), not total column aerosol.
	MISR-JPL	10	23	Urban surface variability and mountainous altitude variability.
	Nes Ziona	124	18	Semi-arid.
	Oyster	6	0	Swampy land and sandy beach (100% pass over ocean).
	Palencia	41	31	?
	Pic du midi	21	47	High altitude station, not total column aerosol.
	Railroad Valley	135	31	Arid, dry lake bed.
	Rimrock	111	44	Prairie, canyon, agricultural, semi-arid area.
	Rogers Dry Lake	106	24	Arid, dry lake bed.
	Saturn Island	90	48	Land surrounded by water
	Seville	160	35	Arid.
X	Shelton	2	0	Site near the multi-channel Platte River in Nebraska.
	Sua Pan	6	27	Arid, dry lake bed. Bright salt pan.
	TABLE MOUNTAIN	31	2	AERONET instrument on mountain (2.2 km altitude) near Mojave desert. Not total column aerosol.
	THALA	66	35	AERONET instrument at 1.1 km altitude in a mountainous arid region. Not total column aerosol.
	Toulon	45	28	Urban surface variability. Marshy water-logged surroundings, with neighboring hills.
	Toulouse	142	39	Urban surface variability.
	Tucson	18	0	Arid and urban surface variability
X	Venise	187	16	Offshore platform. Only limited land strip with Venise urban surface variability and canal.
	Wallops	119	35	Marshes, sandy beaches.
	White Sands	18	14	Dry lake bed, gypsum flakes bright surface.
	Yulin	41	48	Urban surface variability. Also semi-arid, bordering the Mu Us desert.

Table 2b

Excluded	Name	n _{data}	%pass	Probable cause(s) of elevated uncertainty
OCEAN				
	Anmyon	11	41	Possible water sediment in the Yellow Sea.
	Arica	46	37	Cloudy in the morning.
X	Bac_Lieu	2	0	Swampy river delta (also 0% pass over land). Approximately 10 km from ocean.
	BORDEAUX	6	41	Busy sea port.
X	Bragansa	2	0	Known AERONET instrument problem.
X	CEILAP-BA	10	7	Near Buenos Aires. Close to mouth of a wide river turning to estuary with sediments. Far from ocean.
	Che-Ju	17	22	Very mixed aerosol type (dust, pollution, sea salt).
	Chen-Kung Univ	3	0	Uncertain data sampling.
	Dakar	40	45	Dust non-sphericity problem.
	ETNA	3	40	High altitude station, not total column aerosol.
	Dhabi	5	40	Water is not open ocean. UAE Persian Gulf. Complex coastline, possible land masking innacuracy.
	Guadeloup	17	33	Suspected AERONET instrument problem (some time periods)
	IMS-METU-	65	49	Complex coastline, possible land masking innacuracy.
X	Mauna Loa	32	6	High altitude (~3.4 km), not total column aerosol.
	Mont Joli	10	40	Water is not open ocean, just St Lawrence River. Possible land masking innacuracy.
	NCU_Taiwan	7	29	Uncertain data sampling.
	Norfolk State Univ	8	38	Complex coastline, possible land masking innacuracy.
	Oostende	34	43	Busy sea port.
	Rome_Tor_Vergata	10	40	AERONET instrument far from ocean.
	Shirahama	34	47	Complex coastline, possible land masking innacuracy.
	Taipei_CWB	3	0	Uncertain data sampling.
X	UCLA	1	0	AERONET instrument far from ocean.

Table 3: Parameters of the global accuracy ratio ($\%pass$) and linear regression fit of 50x50-km average MODIS level 2 AOT against ± 30 -min average AERONET levels 1.5 and 2.0 AOT.

Data Version	N	$\lambda=470$ nm	$\lambda=550$ nm	$\lambda=660$ nm	$\lambda=870$ nm	N	$\lambda=470$ nm	$\lambda=550$ nm	$\lambda=660$ nm	$\lambda=870$ nm
Using AERONET Level 1.5 AOT						Using AERONET Level 2.0 AOT				
<i>Percent of data within error bounds</i>						<i>Percent of data within error bounds</i>				
T003_Land	8608	58.8	67.3	70.2	N/A	7252	58.3	67.5	70.7	N/A
T004_Land	9740	53.8	53.5	52.8	N/A	3550	52.9	55.0	56.5	N/A
A003_Land	8806	48.1	50.8	51.0	N/A	2787	48.8	55.5	56.8	N/A
T003_Ocean	2750	56.3	62.2	65.6	69.6	2401	57.6	63.3	66.7	70.6
T004_Ocean	2025	49.8	57.0	62.5	66.8	667	53.5	59.7	66.3	69.5
A003_Ocean	1980	54.7	59.5	63.3	67.6	605	58.0	62.8	66.9	71.9
<i>Linear Correlation Coefficient</i>						<i>Linear Correlation Coefficient</i>				
T003_Land		0.81	0.76	0.62	N/A		0.85	0.82	0.71	N/A
T004_Land		0.76	0.68	0.51	N/A		0.80	0.71	0.52	N/A
A003_Land		0.76	0.68	0.51	N/A		0.85	0.81	0.66	N/A
T003_Ocean		0.83	0.81	0.78	0.74		0.91	0.91	0.91	0.89
T004_Ocean		0.92	0.93	0.93	0.93		0.93	0.95	0.95	0.96
A003_Ocean		0.92	0.93	0.93	0.92		0.93	0.93	0.93	0.93
<i>Slope of Regression line</i>						<i>Slope of Regression line</i>				
T003_Land		0.75	0.66	0.55	N/A		0.79	0.75	0.69	N/A
T004_Land		0.73	0.72	0.70	N/A		0.76	0.78	0.79	N/A
A003_Land		0.84	0.75	0.66	N/A		1.01	0.92	0.83	N/A
T003_Ocean		0.78	0.74	0.70	0.59		0.96	0.96	0.97	0.89
T004_Ocean		1.07	1.04	1.01	0.93		1.01	1.00	0.99	0.94
A003_Ocean		0.97	0.93	0.90	0.80		0.95	0.92	0.91	0.82
<i>Intercept of Regression line</i>						<i>Intercept of Regression line</i>				
T003_Land		0.107	0.092	0.086	N/A		0.100	0.078	0.066	N/A
T004_Land		0.122	0.128	0.141	N/A		0.113	0.111	0.117	N/A
A003_Land		0.120	0.136	0.154	N/A		0.067	0.081	0.094	N/A
T003_Ocean		0.047	0.045	0.047	0.047		0.017	0.013	0.014	0.019
T004_Ocean		-0.024	-0.016	-0.004	0.007		-0.007	-0.005	0.001	0.007
A003_Ocean		0.000	0.001	0.007	0.013		0.009	0.008	0.010	0.014

Table 4a: Summary of the regional validation of MODIS AOT with AERONET over land.

Label	Region Name	AERONET Stations Used	MODIS Validation Summary
LAND			
1	NW_America	HJAndrews, Lochiel, Missoula, Rimrock, Saturn_Island	MODIS shows slight to moderate overestimation. T003 and A003 have the same accuracy. T004 has better accuracy than the others.
2	US_Central	BRSN_BAO_Boulder, Cart_Site, Chequamegon, IHOP_Homestead, KONZA_EDC, Sevilleta, Sioux_Falls, White_Sands	MODIS shows slight to moderate overestimation. T004 became more overestimated than T003 because the algorithm for T004 included retrieval over brighter surfaces, which cause overestimation. T004 and A003 show comparable accuracies.
3	US_East	Big_Meadows, BONDVILLE, Brookhaven, CARTEL, CCNY, Columbia_SC, Egbert, GISS, GSFC, Harvard_Forest, MD_Science_Center, Norfolk_State_Univ, Oyster, Penn_State_Univ, Philadelphia, Rochester, SERC, Stennis_Walker_Branch, Wallops	MODIS shows moderate overestimation. T004 is slightly more overestimated than T003 because more bright surfaces were included in the retrieval for T004 than for T003. T004 and A003 show comparable accuracies.
4	Brazil	Alta_Floresta, Balbina, Belterra, CUIABA-MIRANDA, Sao_Paulo, Sao_Paulo_State_Park	There is some balance in negative and positive error distribution for all product versions. The errors are small, with Terra (T003 and T004) showing a net underestimation, and Aqua (A003) the opposite.
5	W_Africa	Banizoumbou, Ilorin, Ougadougou	This region shows moderate underestimation (irrespective of satellite or version), probably because its mix of pollution, smoke, dust, and high cloudiness, causes overfiltering of clouds in MODIS.
6	S_Africa	Bethlehem, Etosha_Pan, Inhaca, Kaoma, Maun_Tower, Mongu, Mwinilunga, Ndola, Pietersburg, Senanga, Skukuza, Solwezi, Sua_Pan, Zambezi	This region shows slight bias toward underestimation, which was moderate with T003, but improved drastically for T004 and A003 because of the adjustment of the single scattering albedo for southern African smoke, which has greater absorption relative to other regions.
7	W_Europe	Avignon, Belsk, BORDEAUX, Bucarest, Creteil, Davos, Fontainebleau, Gerlitz, Gotland, Hamburg, IFT_Leipzig, ISDGM_CNR, Ispra, Lille, Minsk, Modena, Moldova, Munich_Maisach, Oostende, Palaiseau, Pic_du_midi, Rome_Tor_Vergata, Sopot, Tarbes_Etal, The_Hague, Toravere, Toulouse, Villefranche	MODIS seems to be accurate in periods with low to moderate AOT, but overestimates moderately during the summer peak pollution seasons. Overall, T004 and A003 are more overestimated when compared with T003 because of the effect of the inclusion of brighter surfaces in the later (T004 and A003) retrievals.
8	Middle_E	IMS_METU_ERDEMLI, Nes_Ziona	MODIS appears to overestimate always because the area is mostly bright surfaces. The moderate overestimation with T003 increased to high with T004 and A003 because of the inclusion of even brighter surfaces.
9	India	Kanpur	Only one AERONET station is located in this region, with only few monthly averages. Not representative of region. However, there is little to moderate net overestimation overall.
10	Russia	Krasnoyarsk, Tomsk	Only two AERONET stations and few monthly averages, there appears to be a good accuracy here for all the data sets.
11	China	Beijing, Dalanzadgad, Yulin	MODIS appears to overestimate always because the area is mostly bright surfaces with complex aerosol mix, but overestimation increased with T004 and A003 because of the inclusion of even brighter surfaces.
12	Australia	Coleambally, Lake_Argyle	The Australian AERONET stations are relatively new and may still be uncalibrated, thereby causing the overestimation by MODIS due to bright surfaces to appear constantly increasing.

Table 4b: Summary of the regional validation of MODIS AOT with AERONET over ocean.

Label	Region Name	AERONET Stations Used	MODIS Validation Summary
OCEAN			
A	C_Pacific	Coconut_Island, Lanai, Midway_Island, Tahiti	MODIS shows high accuracy here, with T004 and A003 slightly underestimated.
B	M_Atlantic	Capo_Verde, Dahkla, Dakar	The accuracy here is surprisingly good, given that this region is affected by a mix of smoke, dust, and sea salt. However, Terra-MODIS (T003 and T004) shows slight overestimation, and Aqua-MODIS (A003) the opposite.
C	S_Atlantic	Ascension_Island	Only one AERONET station is located here. Not representative of region. However, net result is little to moderate underestimation.
D	Medit_Sea	ETNA, FORTH_CRETE, IMC_Oristano, IMS-METU-ERDEMLI, Lampedusa, Nes_Ziona	MODIS always shows high accuracy here regardless of product version. This is very impressive.
E	N_Indian	MALE	Only one AERONET station. Very limited data sets. No collocated data from Aqua. However, available Terra data seem excellent.
F	Asian_Pacific	Anmyon, Che-Ju, Chen-Kung_Univ, Nauru, NCU_Taiwan, Noto, Okinawa, Shirahama, Taipei_CWB	Data was limited in this region. Mostly moderate underestimation for all data versions. Underestimation probably due to aerosol mixing.

Table 5: Average regional (Aqua - Terra) difference of AOT at 550 nm for the period of June 2002 to December 2003.

Label	Name	Avg^{A-T} AOT550diff
LAND		
1	NW_America	0.035
2	US_Central	0.018
3	US_East	0.036
4	Brazil	0.016
5	W_Africa	-0.012
6	S_Africa	0.020
7	W_Europe	0.007
8	Middle_E	0.016
9	India	0.016
10	Russia	0.063
11	China	0.003
12	Australia	0.010
OCEAN		
A	C_Pacific	-0.005
B	M_Atlantic	-0.004
C	S_Atlantic	-0.004
D	Medit_Sea	0.005
E	N_Indian	-0.004
F	Asian_Pacific	0.001